General Disclaimer

One or more of the Following Statements may affect this Document

- This document has been reproduced from the best copy furnished by the organizational source. It is being released in the interest of making available as much information as possible.

- This document may contain data, which exceeds the sheet parameters. It was furnished in this condition by the organizational source and is the best copy available.

- This document may contain tone-on-tone or color graphs, charts and/or pictures, which have been reproduced in black and white.

- This document is paginated as submitted by the original source.

- Portions of this document are not fully legible due to the historical nature of some of the material. However, it is the best reproduction available from the original submission.

X-621-70-22.
PREPRINT

NASA TM X- 63961

NEUTRAL COMPOSITION AND DENSITY RESULTS FROM THE EXPLORER 32 MASS SPECTROMETERS

C. A. REBER
A. E. HEDIN
J. E. COOLEY
D. N. HARPOLD

MAY 1970

GSFC
GODDARD SPACE FLIGHT CENTER
GREENBELT, MARYLAND

NEUTRAL COMPOSITION AND DENSITY RESULTS FROM THE EXPLORER 32 MASS SPECTROMETERS

ABSTRACT

The magnetic mass spectrometers on the Explorer 32 Aeronomy satellite provided data on the neutral atmospheric constituents in the altitude range 286 kilometers to 1000 kilometers from 26 May to 1 June 1966. Comparison with the Jacchia 1965 model shows good agreement for N_2 densities and the measured atomic oxygen about a factor of five lower than the model. The ion sources of the mass spectrometers were enclosed and coated to enhance recombination of the atomic oxygen; it is likely that significant loss of oxygen occurred on the walls. Using the model to normalize the helium densities allows the determination of the latitudinal gradient for quiet magnetic conditions ($a_p < 16$), $0 \leq \lambda \leq 65°$ in the winter hemisphere:

$$[He] = [He]_m \ (0.85 - 1.1 \times 10^{-2}\lambda)$$

where $[He]$ is the measured helium concentration, $[He]_m$ is the model value, and λ is the latitude. The data for N_2 and O are best fitted with an increase in exospheric temperature of about 160° or a much smaller latitudinal temperature effect than the model predicts, along with a decrease in atomic oxygen density with increasing latitude.

CONTENTS

TABLES

ILLUSTRATIONS

ILLUSTRATIONS (Continued)

NEUTRAL COMPOSITION AND DENSITY RESULTS FROM THE EXPLORER 32 MASS SPECTROMETERS

INTRODUCTION

The Explorer 32 satellite (Atmospheric Explorer B) was launched on 25 May 1966 to provide direct measurements of aeronomic parameters for studying the structure of the upper atmosphere and ionosphere as a function of time, altitude, geographic location, and solar activity. The measurements and studies made were a continuation of those begun with the aeronomy satellite Explorer 17.

The spin-stabilized satellite was a vacuum tight stainless steel sphere 35 inches in diameter with sensors arrayed on the surface (Figure 1). The measurement instruments included three total density gauges, two electrostatic probes, one ion mass spectrometer, and two neutral mass spectrometers. In addition, there were optical and magnetic aspect sensors, magnetic attitude and spin rate control systems, and a tape recorder for data acquisition at locations remote from ground receiving stations. Data were obtained in programmed four minute "turn-ons". Perigee altitude was 286 km, initial apogee was 2700 km, and the inclination of the orbit plane was 64.6°.

The purpose of this paper is to present the data obtained from the neutral mass spectrometers and interpretations of the atmospheric phenomena observed. Electronic malfunctions of the logic of the two spectrometers, possibly

precipitated by exposure to radiation at the higher altitudes, caused one instrument to fail after four days in orbit and the other after seven days.

INSTRUMENTATION

The neutral composition experiment consisted of two double-focusing magnetic mass spectrometers and associated electronics. One (equatorial) was mounted on the equator, normal to the spin axis, and the other (polar) was mounted parallel to the spin axis at the 'top' of the satellite. The instruments were similar to those flown on Explorer 17 (Reber and Hall, 1966) with the exception of the ion source. The Explorer 17 instruments employed a semi-open ion source to minimize surface collisions, and thus loss of atomic oxygen, for incoming ambient particles. Difficulties were experienced, however, in focusing the 1.5 to 12 ev incoming particles which resulted from the 8 km/sec satellite velocity, as well as in correcting for the gas-surface interactions still present. On Explorer 32 the ion source was enclosed in a chamber exposed to the atmosphere through a knife-edged orifice (Figure 2), thus allowing use of the orifice pressure probe theory (Horowitz and LaGow, 1957) for interpreting the data. To facilitate the measurement of atomic oxygen, the surfaces of the ion source and chamber interior were silver plated and oxidized in an atomic oxygen beam to enhance recombination of atomic oxygen (Greaves and Linnett, 1958; Harpold and Reber, 1968). In the altitude range of the satellite, where ambient molecular oxygen density should be less than 5% of

the ambient atomic oxygen density (CIRA, 1965), ambient atomic oxygen can be determined from a combination of the observed (recombined) molecular oxygen in the ion source and remaining atomic oxygen.

In order to detect ions of various mass to charge ratios the spectrometers employed a set of seven different collector cups, rather than varying either the analyzer magnetic field or ion energy, and an electrometer amplifier was switched from one collector to another. The electrometer had two sensitivity ranges, differing by a factor of 100. The noise level, with a 10^{12} ohm feedback resistor, was less than one millivolt, and the total dynamic range was greater than 10^{6}. Two different output signals were provided simultaneously to the telemetry system, one was related linearly to the electrometer output (the so-called biased output) and the other used a logarithmic amplifier to compress the output range to 0 to 5 volts for the telemetry system.

Figure 3 is a photograph of flight data showing the logarithmic outputs from the equatorial and polar instruments. The electronic logic systems for the two sensors could run independently, but were normally synchronized to the spacecraft telemetry clock, thus allowing simultaneous sampling of the various gases by the two systems. The dwell time on a specific mass and sensitivity range was 2.4 seconds to assure complete sampling over the 2.0 second spin period of the satellite. The time for one complete cycle of fifteen logic steps was 36 seconds. The first four steps of the cycle were the rezero operation (to cancel the approximately 1 mv/min zero drift of the electrometer) and the

low and high sensitivity zero levels, then came measurements of the ion currents at m/e 2, 4, and 14 (high sensitivity only) and m/e 28, 32, 16, and 18 (both low and high sensitivity). Every third cycle an eight step calibration voltage staircase was applied to the input of the logarithmic amplifier. Following the calibration, the normally grounded exit slit of the ion source was switched to the input of the electrometer to provide a measure of the total ion current.

For calibration, the spectrometers were placed on an ultra high vacuum system and, after baking at 350° C for 12 hours, a residual pressure in the 10^{-10}torr region was attained. Samples of pure gases (N_2, O_2, H_2, or He) were introduced in small increments through a leak valve and outputs of the spectrometers and a set of Veeco RG 75 pressure gauges were recorded simultaneously. Two separate calibrations were conducted with all four gases and spectrometer sensitivities were consistent to within 2%. The ionization gauges had been previously calibrated against a McCleod absolute pressure gauge using the Florescu method of pressure reduction (Florescu, 1962). Several of the calibrated gauges have been used in the calibration of the omegatron and quadrupole mass spectrometers flown on the Thermosphere Probe rocket series (Spencer et al, 1965) and the neutral mass spectrometer flown on the Geoprobe rocket (Cooley and Reber, 1968). The ion gauges were also compared with the ion gauges used for calibrating the total pressure gauges flown on Explorer 32

(Newton et al, 1968) and a small adjustment (14.5%) in spectrometer sensitivity was made to bring the two types of instruments into agreement.

The mass spectrometer sensitivity for atomic oxygen was obtained from the molecular oxygen calibration and the relative ionization cross sections of O and O_2 (Fite and Brackmann, 1959). As a test of the spectrometer calibration, both air and equal parts of N_2 and O_2 were introduced into the system and measured ratios agreed to within 3% of the known sample ratios.

After calibration, the spectrometers were baked for approximately 20 hours at 250°C on an ion pumped system, then pinched off and held under vacuum by a 0.15 liter/sec ion pump located on the break-off hat. Pumping continued until just prior to launch. After the satellite had been injected into orbit, pyrotechnic chisels on the break-off hats fractured the ceramic seals and the hats were ejected, exposing the inlet orifices to the ambient atmosphere.

DATA ANALYSIS

Equatorial Spectrometer

The basic analysis procedure for the equatorial spectrometer data consisted of transforming the logarithmic amplifier output voltages to electrometer output voltages, fitting the spin modulated data with a standard F(S) type curve, and calculating ambient density using the amplitude of the modulation and the sensitivity determined from laboratory calibrations.

A segment of data for a given mass sample includes 96 values of the biased output voltage and logarithmic amplifier output voltage. A predetermined

number of points at the beginning and end of each data segment were eliminated to avoid electronic switching transients. There were 56 usable points for each segment of mass 2, 4, and 14, and 79 points for each segment of the other masses. For these points, the logarithmic amplifier and biased output voltages were transformed to electrometer output voltages. The function for transforming the logarithmic output to electrometer output was based on the eight calibration voltages telemetered in the middle of each turn-on, and consisted of segments of conic sections, used as interpolation curves, between the calibration points. Electrometer output voltages determined from the biased output and logarithmic amplifier output agreed to within 2% when the electrometer output was large enough to be accurately determined from the biased output.

The relation between ion source number density and ambient number density was taken to be (Horowitz and LaGow, 1957):

$$n_g = n_a (c_a/c_g) F(S) \qquad (1)$$

where

n_g = ion source number density

n_a = ambient number density

c_a = mean speed of ambient particles

c_g = mean speed of particles in ion source

$F(S) = \pi^{1/2} \; S(1 + \text{erf } S) + \exp(-S^2)$

S = ratio of vehicle velocity (normal to orifice) to most probable speed of ambient particles

Equation 1 applies directly for obtaining $n_a(He)$ from the mass 4 peak, $n_a(N_2)$ from the mass 28 or 14 peak, and atomic oxygen from the mass 16 peak (after correcting for ion contributions from electron bombardment of molecular oxygen in the source). Assuming the mass 32 peak to be due to recombined atomic oxygen in the source, the related ambient atomic oxygen (which must be added to that determined from the mass 16 peak) was found by using mass 16 in calculating c_a and S, mass 32 in calculating c_g, and introducing a factor of 1/2 on the right side of Equation 1 to account for the atomic flux into and molecular flux out of the chamber. The ambient atomic hydrogen density was calculated using the mass 2 peak only, and assuming complete recombination.

In actual practice, the method of least squares was used to fit the electrometer output voltages with the formula:

$$y = (q_1 + q_2 \, F(S_m \cos\omega (t - q_3))) \, R(t - q_3) \qquad (2)$$

where

S_m = maximum speed ratio in spin cycle

ω = angular spin rate of satellite

t = time of measured output voltage

y = calculated output voltage

q_1, q_2 = parameters to be determined from the least squares fit

$R(t - q_3)$ = repeller correction factor

Comparing Equation 1 and Equation 2, it is seen that q_1 is proportional to a constant gas background, q_2 is proportional to the ambient density, and q_3 is

the time of maximum output voltage. The constant of proportionality is the spectrometer sensitivity determined in the laboratory times the ratio c_a/c_g. Minor corrections were made for slight changes in the electron emission current, electronics temperatures, and high voltage values recorded during the flight. A major correction for variations in repeller voltage was sometimes required, as indicated in Equation 2 and discussed in detail in the following paragraph.

The voltage on the ion source repeller electrode was found to decrease by up to 35 volts during several turn-ons, with maximum deviation at maximum ram and no deviation at the anti-ram point. The amplitude of the repeller voltage variation was closely correlated with electron density as determined by the electron-temperature probe experiment (Brace, 1968). Apparently the variation was caused by electrons, drawn to the repeller electrode, flowing through the high impedance voltage divider string. Since the housekeeping data output reported the repeller voltage only once for every 64 main data points, the form of the repeller variation over a spin cycle was determined by superposition of data from a large number of cycles. The repeller voltage variation with time in the spin cycle was then approximated by several straight lines to provide a voltage at any required time (Figure 4). The effect of the repeller variation on spectrometer sensitivity was investigated in the laboratory using the backup flight instrument. The spectrometer sensitivity as a function of repeller voltage was determined for each mass peak and approximated, for

calculation purposes, by a second degree polynomial. (Figure 5). The repeller correction factor indicated in Equation 2 is thus a combination of sensitivity as a function of repeller voltage and repeller voltage as a function of time.

In Figure 6 the measured data points for a segment of mass 28 data taken near perigee are compared to the curve determined from the least squares fit. The agreement is satisfactory for data taken below 400 km. However, above 500 km the measured points do not follow an F(S) curve (Figure 7). Thus above 400 to 500 km, the amplitude of the modulation does not represent ambient gas density. In fact, the amplitude varies with height in a manner similar to the variation of electron density with height. Considering also the shape of the modulation, namely a significant signal at the 90° points, it is speculated that the modulation is the result of ions or neutrals released from surfaces near or in the ion source by ambient electrons drawn into the source region by the repeller electrode. The gas modulation curve at the higher altitudes is also very similar to the variation of repeller voltage with spin angle noted earlier. These spin modulation anomalies are apparent also on the mass 14, 16, and 32 peaks beginning at about the same altitude range. The mass 4 peak data show no detectable deviations from F(S) at any altitude. The mass 2 peak appears to have a spin modulation shape at all altitudes which is similar to the mass 28 peak modulation above 500 km, however the shape is less well defined than the mass 28 peak because of a large initial transient. There is no detectable

maximum signal at maximum ram above 1500 km for any of the masses, but for masses 16, and 28 there is a small maximum which appears at the time the sun shines most directly into the source.

The accuracy of the ambient densities from the equatorial spectrometer is primarily limited by the uncertainty in the repeller correction factor. A minimum uncertainty of 10% was assumed, and any deviation of the sensitivity from nominal because of the repeller correction was taken to have an accuracy of 50%. On this basis, typical density uncertainties as a result of the repeller correction were: 12% for mass 2; 15% for masses 4, 14, and 32; and 25% for masses 28 and 16. On some turn-ons the repeller correction became very large, particularly for masses 28 and 32, and these data have been excluded from data summaries given later. Less important sources of density uncertainties were the 2 to 3% from the least squares fit and digital nature of the data transmission (except 12% for mass 4), less than 4% from uncertainty in angle of attack, and 2 to 3% from uncertainty in the logarithmic amplifier calibration.

Polar Spectrometer

The analysis procedure for the polar spectrometer included transforming the logarithmic amplifier output voltage to electrometer output voltage, determining source density from the average output voltage, subtracting background density, and calculating ambient density using an appropriate F(S) value in Equation 1.

altitude data. The background varied with time from the beginning of each filament turn-on, so an appropriate value was used for each cycle (Figure 8). Because of a wide spread in the high altitude source densities, the background is taken to be accurate to ±50%.

The ambient density was calculated from the net source density using Equation 1, with the same assumptions for mass 2 and 32 data as described for the equatorial spectrometer.

The accuracy of the ambient densities from the polar spectrometer is primarily limited by the uncertainty in the repeller correction factor and the angle of attack. Density uncertainties resulting from the repeller correction were typically 15 to 20% for all masses. Density error due to angle of attack uncertainty was about 10%. For the data below 500 km the error from the background correction was generally less than 1%, except 10 to 20% for mass 2 and 16. Other sources of density uncertainties were 2 to 3% from the least squares fit and digital nature of data transmission, about 3% from the log calibration, and 1 to 3% from the electrometer zero subtraction for masses 2 and 4.

Ambient Densities

The ambient densities obtained from the two spectrometers were combined in a weighted average, with weights equal to the inverse square of the net density uncertainties for each spectrometer. The total atomic oxygen density was calculated for each spectrometer separately, by adding the results from the mass 32 and 16 peaks, and the total densities for each spectrometer were then

averaged. For hydrogen, helium, and total oxygen, there were only two values to be averaged, one from each spectrometer. For molecular nitrogen, the density from the mass 14 peak was interpolated to the high sensitivity mass 28 peak time and averaged with the high sensitivity result, giving a total of four values to be averaged. If the high sensitivity output was saturated, the low sensitivity value was used. The uncertainties in the final density were taken as the larger of two determinations, one the standard error of the mean determined from the variance of the numbers averaged, and the second by applying the standard method of propagating errors from the individual densities through the averaging formula. The densities for He and N_2 were relatively consistent from the two spectrometers and typical net uncertainties ranged from 15 to 25% for He and about 10% for N_2. Hydrogen densities from the equatorial spectrometer were about a factor of two above those from the polar spectrometer, and net uncertainties ranged from 15 to 60% because of the spread. Polar spectrometer atomic oxygen densities were from 40 to 100% above equatorial spectrometer values and net uncertainties ranged from 15 to 35%. Atomic oxygen results have an additional uncertainty because of the unknown amount of absorption possible on the spectrometer walls, thus densities given are likely to be below the true density. Finally, when taken as absolute number densities, there is an additional contribution to all the density uncertainties of about 16% based on determination of absolute pressure and spectrometer sensitivity in laboratory calibration. The altitudes to which the data are assigned are precise to ± 1 kilometer.

DATA

The relationship between local time, altitude, and latitude for the first week of operation of Explorer 32 is shown in Figures 9 and 10. It can be seen that most of the useful data were acquired between 0700 and 1500 hrs local time and from the equator north to about 65°.

Tables 1a-1d contain data for all altitudes below 625 km and include the turn-on number (TO), date, greenwich mean time (UT), altitude (ALT), latitude (LAT), longitude (LONG), local solar time (LT), number densities from the equatorial spectrometer (MS1) and polar spectrometer (MS2), average density (AVG DEN), and the percent errors (ERR). The densities and uncertainties were determined as described in the last section for hydrogen from mass 2, helium from mass 4, molecular nitrogen from mass 14 and 28, and atomic oxygen from mass 16 and 32. The 16% uncertainty in absolute density, due to the uncertainty in laboratory calibrations, has not been included in the figures given in the tables. The average densities are plotted as a function of altitude in Figures 11a-11d.

The densities from each cycle were also interpolated to a common altitude (that of mass 28) in order to calculate total mass density and mean molecular weight. These are tabulated in Table 2; total mass density is plotted as a function of altitude in Figure 12. The uncertainty in the total mass density ranges from 25 to 30%.

DISCUSSION AND CONCLUSIONS

The ratio of total mass density to density derived from the pressure gauges on Explorer 32 (Newton, 1968) is shown in Figure 13. The ratio is relatively consistent between turn-ons, certainly within overall experimental error. However, as a whole, the mass spectrometer densities are 40 to 50% below the pressure gauge values; no satisfactory explanation for this difference has been found. A comparison of ion gauges used for calibrating the mass spectrometers and those used for calibrating the flight pressure gauges was made and the spectrometer sensitivities were adjusted slightly to be consistent with the flight pressure gauges. As discussed below, the measured atomic oxygen density may well be too low. A factor of four higher oxygen density would eliminate the total density discrepancy.

The ratios of measured number densities to the Jacchia 1965 model densities (Jacchia, 1965) are shown in Figures 14a and b for N_2 and O. Atomic oxygen is a factor of three to six lower than the model. It is very likely that there was a significant loss of this reactive gas on the walls of the thermalization chamber. (The nature of these surfaces and their treatment is discussed by Harpold and Reber (1968).) Preliminary analysis of data from the mass spectrometer on the OGO-6 (with a gold antechamber surface) indicates a stabilization time of several weeks for atomic oxygen; during this time the indicated amount of oxygen increased by more than a factor of five. It is not clear from the Explorer 32 data that the surfaces stopped absorbing oxygen during the

period of operation. It should be noted also that the polar spectrometer gave atomic oxygen densities a factor of 1.4 to 2 above the equatorial spectrometer values, a discrepancy for which there is no ready explanation.

The molecular nitrogen measured is in general higher than that predicted by the Jacchia model, and the divergence increases with increasing altitude and/or latitude. Comparing the behavior of N_2 and O as a function of altitude (Figure 14b) it can be seen that a change in temperature alone cannot bring the two gases into agreement. It appears that the data can be fitted by a decrease in the model latitudinal temperature gradient (or an increase in the exospheric temperature of about 160°) and a decrease in the atomic oxygen density with increasing latitude. This is in qualitative agreement with data obtained in June 1969 from the quadrupole mass spectrometer flown on OGO-6 (Reber, et al., 1970). The data cannot be fitted with a model using constant boundary conditions, vertical diffusive equilibrium and horizontal temperature gradients alone.

The helium densities (Figure 15) also show distinct variation with latitude and/or local time. Because of the limited data and close correlation between local time and latitude (Figure 10), it is not possible to determine which factor is more significant from the data alone. However, if the variation is taken to be latitudinal, it is in qualitative agreement with trends noted in Explorer 17 data (Reber and Nicolet, 1965), the "winter helium bulge" concept suggested to explain satellite drag anomalies (Keating and Prior, 1968), recent rocket

measurements (summarized by Krankowsky, et al., 1968) which show helium densities during northern hemisphere winter to be an order of magnitude higher than those during spring and summer, and recent data acquired with the quadrupole mass spectrometer flown on OGO-6 (Reber, et al., 1970).

By choosing turn-ons with a_p less than 16 and assuming a linear variation with latitude we obtain the distribution of helium in the Northern (summer) hemisphere for quiet geomagnetic conditions:

$$[He] = [He]_m \ (0.85 - 1.1 \times 10^{-2} \lambda) \qquad (4)$$

where $[He]$ represents an average of the data, $[He]_m$ is the helium density from the Jacchia model, and λ is the latitude. Two turn-ons, 15 and 73, during geomagnetic disturbances (Figure 16), have anomalously low helium densities. Two other turn-ons, 18 and 20, near the end of the same storm as turn-on 15 show no significant anomalies, while turn-on 14 (at the onset of the storm) indicates a low density. It appears that the effect of a geomagnetic disturbance on the helium distribution is primarily associated with the onset of the storm and dissipates within a few hours of the end of a storm. (Atomic oxygen is also low during turn-on 15 by approximately a factor of two from densities measured during undisturbed times at the same altitude. The geophysical significance is not entirely clear from the sample of one, however, as there may have been a time dependent adsorption phenomena causing oxygen to appear low during the early turn-ons.)

The hydrogen densities (Figure 11d) are included for completeness, but their geophysical significance is not clear. The scatter in the data results from

the individual points taken during a spin cycle being poorly fit by an F(S) type curve. Taken at face value, the densities are two orders of magnitude larger than Cira 1965 model values and decrease with altitude much faster than the model values. It appears that the current detected as hydrogen (and previously reported, Reber, et al., 1968) was, in fact, generated by gas-surface reactions in the ion source in a manner which resembled the spin modulation effect due to ambient hydrogen.

In summary, comparison of the measured densities in the northern (summer) hemisphere with predictions from the 1965 Jacchia model atmosphere indicates horizontal and temporal variations not properly reproduced in the model. These include (1) a decrease in helium density with latitude, (2) a similar but smaller effect for atomic oxygen, (3) a lower latitudinal temperature gradient (or higher exospheric temperature) and (4) a decrease in helium at the onset of a geomagnetic disturbance.

ACKNOWLEDGMENTS

The authors gratefully acknowledge the contributions of Jack E. Richards and Chester A. Clark for their valuable assistance in the preparation of the experiment, and to Georgiann R. Batluck for her assistance in processing and reducing the data.

REFERENCES

CIRA 1965, "COSPAR International Reference Atmosphere," North Holland Publishing Co., Amsterdam, 1965.

Brace, L. H., private communication, 1968.

Cooley, J. E., and C. A. Reber, "Neutral Atmosphere Composition Measurement Between 133 and 533 Kilometers from the Geoprobe Rocket Mass Spectrometer," NASA X-621-69-260.

Fite, W. L., and R. T. Brackman, "Ionization of Atomic Oxygen on Electron Impact," Phys. Rev., 113, 815, 1959.

Florescu, N. A., "Reproducible Low Pressure and Their Application to Gauge Calibration," Trans. 8th Vac. Symp., 504, 1962.

Jacchia, L. G., "Static Diffusion Models of the Upper Atmosphere with Empirical Temperature Profiles," Smithsonian Contributions to Astrophysics, Vol. 8, No. 9, 1965.

Greaves, J. C., and J. W. Linnet, "The Recombination of Oxygen Atoms at Surfaces, "Trans. Faraday Soc., 54, 1323, 1958.

Harpold, D. N., and C. A. Reber, "A Mass Spectrometric Technique for Measurement of Atomic Oxygen in the Earth's Upper Atmosphere," NASA X-621-68-409, 1968.

Horowitz, R., and H. E. LaGow, "Upper Air Pressure and Density Measurements from 90-220 km with the Viking 7 Rocket," J. Geophys. Res., 62, 57, 1957.

Keating, G. M., and E. J. Prior, "The Winter Helium Bulge," Space Res. VIII, 982, 1968.

Krankowsky, D., W. T. Kasperzak, and A. O. Nier, "Mass Spectrometric Studies of the Composition of the Lower Thermosphere During Summer 1967," J. Geophys. Res., 73, 7291, 1968.

Newton, G. P., private communication, 1968.

Reber, C. A., J. E. Cooley, and D. N. Harpold, "Upper Atmosphere Hydrogen and Helium Measurements from the Explorer 32 Satellite," Space Res. VIII, 993, 1968.

Reber, C. A., and L. G. Hall, "A Double Focusing Magnetic Mass Spectrometer for Satellite Use," NASA TN D-3211, 1966.

Reber, C. A., and M. Nicolet, "Investigation of the Major Constituents of the April-May 1963 Heterosphere by the Explorer XVII Satellite," Planet Space Sci., 13, 617, 1965.

Reber, C. A., D. N. Harpold, A. E. Hedin, N. W. Spencer, G. R. Carignan and D. R. Taeusch, "Neutral Atmospheric Composition Data from the Quadrupole Mass Spectrometer," Presented at Spring AGU meeting, 1970.

Reber, C. A., H. G. Mayr and P. B. Hays, "Thermospheric Wind Effects on the Global Distribution of Helium," Presented at Spring AGU meeting, 1970.

Reber, C. A., G. R. Carignan, N. W. Spencer, D. N. Harpold, A. E. Hedin, and R. Horowitz, "The Horizontal Distribution of Helium in the Earth's Upper Atmosphere," Presented at COSPAR, 1970.

Spencer, N. W., L. H. Brace, G. R. Carignan, D. R. Taeusch, and H. B. Niemann, "Electron and Molecular Nitrogen Temperature and Density in the Thermosphere," J. Geophy. Res., 70, 2665, 1965.

Table Ia ATOMIC HYDROGEN DENSITY(NUM/CM3)

	DATE	UT (HRS)	ALT (KM)	LAT (DEG)	LONG (DEG)	LT (HRS)	MS1 DEN 2 PEAK	ERR (%)	MS2 DEN 2 PEAK	ERR (%)	AVG DEN	ERR (%)
8	5/25/66	1.935	586.	63.8	-164.2	14.99	3.06E 06	15.	7.58E 05	40.	1.56E 06	70.
		1.945	616.	63.1	-159.3	15.33	3.04E 06	13.	5.82E 05	66.	1.80E 06	68.
17	5/26/66	7.373	548.	5.2	-349.9	8.05	2.41E 06	15.	8.69E 05	34.	1.50E 06	50.
		7.383	520.	7.4	-349.0	8.12	3.54E 06	14.	1.20E 06	30.	2.02E 06	55.
		7.393	494.	9.5	-348.1	8.19	3.47E 06	19.	1.61E 06	24.	2.11E 06	39.
		7.410	453.	13.2	-346.5	8.31	9.60E 06	14.	2.11E 06	20.	2.81E 06	77.
		7.420	431.	15.4	-345.6	8.38	1.06E 07	15.	2.76E 06	17.	3.43E 06	64.
		7.430	410.	17.6	-344.6	8.46	6.81E 06	19.	4.04E 06	16.	4.59E 06	24.
14	5/26/66	13.150	621.	-0.2	-79.8	7.83	1.85E 06	14.	6.25E 05	68.	1.50E 06	37.
		13.160	591.	2.0	-79.0	7.89	2.62E 06	13.	9.48E 05	44.	1.93E 06	43.
		13.176	543.	5.5	-77.5	8.01	0.0	0.	1.75E 06	27.	1.75E 06	27.
		13.186	515.	7.7	-76.6	8.08	5.88E 06	15.	2.39E 06	22.	3.33E 06	46.
		13.196	489.	9.9	-75.7	8.15	9.60E 06	13.	2.84E 06	20.	4.02E 06	64.
15	5/26/66	15.249	298.	36.2	-91.2	9.17	8.93E 06	12.	4.28E 06	19.	6.06E 06	37.
		15.259	293.	38.4	-89.7	9.28	6.94E 06	12.	3.10E 06	21.	4.57E 06	41.
		15.276	288.	41.9	-86.8	9.49	5.88E 06	13.	2.59E 06	23.	3.87E 06	41.
		15.286	288.	44.0	-84.9	9.63	6.85E 06	12.	2.65E 06	23.	4.05E 06	49.
		15.296	290.	46.1	-82.8	9.78	6.56E 06	13.	0.0	0.	6.56E 06	13.
9	5/27/66	1.122	531.	64.6	-166.0	14.05	1.68E 06	15.	9.81E 05	60.	1.58E 06	16.
		1.132	559.	64.3	-160.7	14.42	1.46E 06	14.	8.23E 05	82.	1.41E 06	14.
		1.142	588.	63.8	-155.5	14.77	1.37E 06	15.	8.28E 05	83.	1.33E 06	15.
20	5/27/66	2.693	602.	1.1	-284.2	7.75	2.10E 06	13.	1.60E 06	28.	1.96E 06	12.
		2.703	572.	3.2	-283.3	7.82	2.02E 06	17.	2.22E 06	26.	2.07E 06	14.
		2.713	544.	5.3	-282.4	7.88	9.68E 06	16.	3.04E 06	22.	4.06E 06	59.
		2.730	499.	9.0	-280.9	8.00	7.03E 06	16.	4.89E 06	19.	5.75E 06	18.
		2.740	474.	11.1	-280.0	8.07	2.50E 07	17.	5.74E 06	19.	6.99E 06	68.
		2.750	450.	13.3	-279.1	8.14	1.21E 07	21.	6.82E 06	20.	7.98E 06	27.
21	5/27/66	10.667	307.	52.2	-7.7	10.15	4.74E 06	12.	1.77E 06	25.	2.95E 06	49.
		10.677	316.	54.0	-4.8	10.36	2.97E 06	15.	1.89E 06	29.	2.54E 06	21.
		10.687	327.	55.7	-1.7	10.58	2.02E 06	14.	1.97E 06	28.	2.01E 06	13.
		10.704	348.	58.3	4.2	10.99	3.22E 06	12.	1.53E 06	35.	2.64E 06	30.
		10.714	363.	59.7	8.2	11.26	1.84E 06	17.	1.75E 06	33.	1.81E 06	15.
		10.724	380.	61.0	12.4	11.55	5.03E 06	16.	1.65E 06	34.	2.80E 06	57.
28	5/27/66	14.436	314.	31.6	-85.4	8.74	1.12E 07	18.	4.62E 06	20.	5.82E 06	44.
		14.446	305.	33.8	-84.0	8.84	7.84E 06	16.	4.19E 06	21.	5.35E 06	32.
		14.456	298.	36.0	-82.5	8.95	3.77E 06	17.	3.38E 06	22.	3.60E 06	13.
		14.473	291.	39.6	-79.9	9.15	6.03E 06	13.	2.45E 06	23.	3.75E 06	46.
		14.483	288.	41.7	-78.1	9.28	4.39E 06	15.	2.48E 06	25.	3.39E 06	28.
		14.493	288.	43.8	-76.2	9.41	8.78E 06	14.	2.50E 06	23.	3.58E 06	66.
33	5/27/66	22.033	601.	1.0	143.2	7.58	2.35E 05	50.	0.0	0.	2.35E 05	50.
		22.043	571.	3.1	-20.2	7.65	4.33E 05	31.	0.0	0.	4.33E 05	31.

Table Ia (Continued) ATOMIC HYDROGEN DENSITY(NUM/CM3)

TO	DATE	UT (HRS)	ALT (KM)	LAT (DEG)	LONG (DEG)	LT (HRS)	MS1 DEN 2 PEAK	ERR (%)	MS2 DEN 2 PEAK	ERR (%)	AVG DEN	ERR (%)
39	5/28/66	13.723	294.	48.4	-62.4	9.56	4.20E 06	12.	2.51E 06	22.	3.40E 06	25.
		13.733	300.	50.4	-60.0	9.74	3.08E 06	15.	2.55E 06	24.	2.89E 06	13.
		13.743	308.	52.2	-57.3	9.92	8.13E 06	14.	2.34E 06	25.	3.58E 06	66.
		13.760	324.	55.2	-52.3	10.27	3.93E 06	12.	1.80E 06	31.	3.06E 06	34.
		13.770	336.	56.8	-49.0	10.50	3.24E 06	12.	2.12E 06	27.	2.88E 06	18.
		13.780	350.	58.3	-45.4	10.76	2.05E 06	16.	2.08E 06	28.	2.06E 06	14.
42	5/28/66	21.539	398.	61.4	-152.7	11.36	3.33E 06	14.	1.64E 06	30.	2.50E 06	34.
		21.549	408.	62.4	-148.0	11.68	2.66E 06	13.	1.19E 06	44.	2.20E 06	31.
		21.559	428.	63.3	-143.0	12.03	3.00E 06	12.	1.26E 06	45.	2.49E 06	32.
		21.575	466.	64.3	-134.2	12.63	1.38E 06	16.	1.22E 06	47.	1.36E 06	15.
		21.585	490.	64.6	-128.8	13.00	2.16E 06	13.	0.0	0.	2.16E 06	13.
		21.595	515.	64.7	-123.3	13.38	1.64E 06	14.	8.63E 05	67.	1.53E 06	18.
46	5/29/66	1.494	601.	63.6	-165.7	14.45	6.25E 05	21.	5.85E 05	85.	6.22E 05	20.
47	5/29/66	6.906	607.	0.3	5.5	7.27	9.12E 04	125.	0.0	0.	9.12E 04	125.
		6.916	577.	2.4	6.3	7.34	3.52E 05	34.	0.0	0.	3.52E 05	34.
		6.926	548.	4.6	7.2	7.41	3.37E 05	35.	7.05E 05	79.	3.52E 05	33.
		6.943	503.	8.2	8.7	7.52	6.54E 05	22.	2.89E 05	150.	6.18E 05	22.
		6.953	478.	10.3	-269.2	7.59	8.17E 05	20.	0.0	0.	8.17E 05	20.
		6.963	454.	12.5	-349.5	7.67	0.0	0.	7.17E 05	61.	7.17E 05	61.
48	5/29/66	9.050	290.	45.9	2.2	9.20	4.65E 06	13.	2.66E 06	22.	3.68E 06	27.
		9.060	294.	47.9	4.4	9.35	4.06E 06	14.	2.57E 06	23.	3.54E 06	29.
		9.076	304.	51.1	8.5	9.64	3.74E 06	16.	2.43E 06	25.	3.10E 06	21.
		9.086	312.	53.0	11.3	9.84	5.12E 06	12.	2.26E 06	26.	3.61E 06	40.
		9.096	322.	54.7	14.3	10.05	4.50E 06	12.	2.67E 06	23.	3.69E 06	25.
57	5/30/66	11.910	620.	-0.8	-73.9	6.99	1.56E 05	70.	0.0	0.	1.56E 05	70.
		11.920	589.	1.3	-73.0	7.05	3.83E 05	31.	0.0	0.	3.83E 05	31.
		11.930	560.	3.4	-72.1	7.12	4.61E 05	28.	0.0	0.	4.61E 05	28.
59	5/30/66	13.972	331.	27.4	-90.5	7.94	3.16E 06	12.	0.0	0.	3.16E 06	12.
		13.982	320.	29.6	-89.2	8.03	2.81E 06	12.	0.0	0.	2.81E 06	12.
		13.992	310.	31.8	-87.9	8.13	2.93E 06	14.	0.0	0.	2.93E 06	14.
		14.009	298.	35.5	-85.5	8.31	2.85E 06	14.	0.0	0.	2.85E 06	14.
		14.019	293.	37.7	-83.9	8.42	4.04E 06	12.	0.0	0.	4.04E 06	12.
		14.029	289.	39.8	-82.3	8.54	3.96E 06	13.	0.0	0.	3.96E 06	13.
68	5/31/66	9.423	304.	51.0	-3.1	9.21	5.35E 06	17.	0.0	0.	5.35E 06	17.
		9.433	313.	52.9	-0.4	9.41	4.61E 06	14.	0.0	0.	4.61E 06	14.
		9.443	323.	54.6	2.6	9.62	4.86E 06	13.	0.0	0.	4.86E 06	13.
		9.470	359.	58.9	11.9	10.26	8.47E 06	16.	0.0	0.	8.47E 06	16.
		9.480	375.	60.2	16.0	10.54	2.90E 06	16.	0.0	0.	2.90E 06	16.
73	5/31/66	21.089	386.	61.0	-157.0	10.63	1.55E 06	15.	0.0	0.	1.55E 06	15.
		21.099	405.	62.1	-152.4	10.94	1.31E 06	14.	0.0	0.	1.31E 06	14.
		21.109	426.	63.0	-147.5	11.27	7.61E 05	20.	0.0	0.	7.61E 05	20.
		21.125	463.	64.1	-138.9	11.86	2.21E 06	13.	0.0	0.	2.21E 06	13.
		21.135	487.	64.5	-133.5	12.23	2.68E 06	12.	0.0	0.	2.68E 06	12.
		21.145	512.	64.6	-128.0	12.61	2.61E 06	12.	0.0	0.	2.61E 06	12.

Table IIb HELIUM DENSITY(NUM/CM3)

TO	DATE	UT (HRS)	ALT (KM)	LAT (DEG)	LONG (DEG)	LT (HRS)	MS1 DEN 4 PEAK	ERR (%)	MS2 DEN 4 PEAK	ERR (%)	AVG DEN	ERR (%)
8	5/26/66	1.936	588.	63.7	-163.8	15.01	2.93E 05	38.	2.74E 05	25.	2.79E 05	21.
		1.946	618.	63.0	-159.0	15.35	2.44E 05	42.	2.32E 05	26.	2.35E 05	22.
1	5/26/66	7.374	546.	5.3	-349.8	8.05	9.00E 05	23.	1.09E 06	16.	1.01E 06	13.
		7.384	518.	7.5	-348.9	8.12	1.06E 06	22.	1.15E 06	15.	1.12E 06	13.
		7.394	492.	9.7	-348.0	8.19	1.01E 06	23.	1.23E 06	16.	1.14E 06	13.
		7.410	452.	13.3	-346.5	8.31	1.27E 06	21.	1.35E 06	18.	1.31E 06	14.
		7.420	429.	15.5	-345.5	8.39	1.45E 06	19.	1.36E 06	19.	1.40E 06	14.
		7.430	408.	17.8	-344.5	8.46	1.42E 06	17.	1.43E 06	20.	1.43E 06	13.
4	5/26/66	13.150	619.	-0.0	-79.8	7.83	8.92E 05	22.	1.13E 06	16.	1.02E 06	13.
		13.160	589.	2.1	-78.9	7.90	7.62E 05	23.	1.16E 06	17.	9.38E 05	21.
		13.177	541.	5.7	-77.5	8.01	9.58E 05	22.	1.17E 06	18.	1.06E 06	14.
		13.187	514.	7.8	-76.6	8.08	9.74E 05	21.	1.22E 06	19.	1.08E 06	14.
		13.197	488.	10.0	-75.7	8.15	1.04E 06	19.	1.21E 06	20.	1.11E 06	14.
5	5/26/66	15.250	298.	36.4	-91.1	9.17	7.40E 05	20.	7.47E 05	22.	7.43E 05	15.
		15.260	293.	38.5	-89.6	9.29	5.34E 05	23.	7.59E 05	20.	6.22E 05	18.
		15.277	288.	42.1	-86.6	9.50	6.75E 05	22.	5.92E 05	21.	6.26E 05	15.
		15.287	288.	44.2	-84.7	9.64	0.0	0.	5.48E 05	20.	5.48E 05	20.
		15.297	290.	46.2	-82.6	9.79	5.46E 05	23.	5.59E 05	20.	5.53E 05	15.
8	5/27/66	1.123	533.	64.6	-165.7	14.08	4.04E 05	28.	3.78E 05	33.	3.93E 05	21.
		1.133	561.	64.3	-160.3	14.44	4.59E 05	26.	4.43E 05	31.	4.52E 05	20.
		1.143	590.	63.8	-155.2	14.80	3.34E 05	30.	4.37E 05	34.	3.66E 05	23.
0	5/27/66	2.694	600.	1.2	-284.1	7.75	1.07E 06	19.	1.36E 06	20.	1.17E 06	14.
		2.704	570.	3.3	-283.2	7.82	1.48E 06	19.	1.72E 06	19.	1.58E 06	14.
		2.714	542.	5.5	-282.4	7.89	1.56E 06	18.	1.84E 06	20.	1.66E 06	13.
		2.731	497.	9.1	-280.9	8.00	1.75E 06	20.	2.01E 06	22.	1.85E 06	15.
		2.741	472.	11.3	-280.0	8.08	1.67E 06	34.	2.04E 06	22.	1.90E 06	19.
		2.751	448.	13.5	-279.0	8.15	4.74E 06	73.	2.10E 06	22.	2.15E 06	21.
5	5/27/66	10.668	307.	52.3	-7.5	10.17	1.52E 06	17.	1.83E 06	20.	1.63E 06	13.
		10.678	317.	54.1	-4.6	10.37	1.50E 06	18.	1.71E 06	20.	1.58E 06	13.
		10.688	327.	55.8	-1.4	10.59	1.58E 06	18.	1.62E 06	20.	1.60E 06	14.
		10.705	349.	58.4	4.5	11.00	1.46E 06	19.	1.39E 06	21.	1.43E 06	14.
		10.715	364.	59.8	8.4	11.28	1.23E 06	19.	1.38E 06	21.	1.29E 06	14.
		10.725	381.	61.1	12.7	11.57	1.22E 06	19.	1.28E 06	21.	1.24E 06	14.
8	5/27/66	14.437	313.	31.7	-85.3	8.75	2.37E 06	61.	2.07E 06	22.	2.10E 06	21.
		14.447	304.	33.9	-83.9	8.85	2.49E 06	41.	2.12E 06	22.	2.18E 06	19.
		14.457	298.	36.1	-82.4	8.96	1.99E 06	28.	1.95E 06	22.	1.97E 06	17.
		14.473	290.	39.7	-79.7	9.16	2.37E 06	16.	1.98E 06	21.	2.19E 06	13.
		14.483	288.	41.9	-78.0	9.29	1.75E 06	14.	1.93E 06	21.	1.80E 06	12.
		14.493	288.	43.9	-76.1	9.42	1.73E 06	15.	1.69E 06	21.	1.72E 06	12.
3	5/27/66	22.033	599.	1.1	143.3	7.58	7.77E 05	22.	1.29E 06	17.	9.72E 05	26.
		22.043	569.	3.3	-62.4	7.65	1.12E 06	21.	1.36E 06	18.	1.24E 06	14.

Table Ic NITROGEN DENSITY(NUM/CM3)

TO	DATE	UT (HRS)	ALT (KM)	LAT (DEG)	LONG (DEG)	LT (HRS)	MS1 DEN 14 PEAK	ERR (%)	MS1 DEN 28 PEAK	ERR (%)	MS2 DEN 14 PEAK	ERR (%)	MS2 DEN 28 PEAK	ERR (%)	AVG DEN	ERR (%)
8	5/26/66	1.937	594.	63.6	-162.9	15.08	6.27E 06	15.	3.52E 06	16.	2.23E 06	31.	3.11E 06	36.	3.57E 06	21.
		1.947	624.	62.9	-158.0	15.41	0.0.	0.	2.54E 06	15.	0.0	0.	2.17E 06	41.	2.49E 06	14.
11	5/26/66	7.375	540.	5.8	-349.7	8.07	4.76E 06	16.	3.47E 06	16.	0.0	0.	2.39E 06	40.	3.64E 06	16.
		7.385	513.	7.9	-348.8	8.13	6.29E 06	16.	4.51E 06	17.	0.0	0.	2.25E 06	33.	4.00E 06	28.
		7.395	487.	10.1	-347.9	8.20	1.09E 07	14.	5.67E 06	18.	3.45E 06	17.	2.52E 06	26.	3.93E 06	31.
		7.412	447.	13.8	-346.3	8.33	1.08E 07	19.	1.06E 07	22.	0.0	0.	3.89E 06	22.	5.41E 06	37.
		7.422	425.	16.0	-345.3	8.40	2.10E 07	18.	2.09E 07	35.	0.0	0.	5.60E 06	24.	7.79E 06	49.
		7.432	404.	18.2	-344.3	8.48	2.54E 07	23.	5.79E 07	60.	0.0	0.	8.70E 06	32.	1.20E 07	43.
14	5/26/66	13.152	613.	0.4	-79.6	7.84	1.94E 06	15.	3.08E 06	15.	1.15E 06	56.	5.78E 05	149.	2.00E 06	20.
		13.162	583.	2.5	-78.8	7.91	4.69E 06	16.	4.17E 06	16.	2.04E 06	28.	1.20E 06	56.	2.86E 06	28.
		13.179	535.	6.1	-77.3	8.03	5.23E 06	18.	7.25E 06	19.	3.79E 06	17.	2.31E 06	28.	3.79E 06	22.
		13.189	509.	8.3	-76.4	8.09	9.74E 06	20.	1.01E 07	22.	5.13E 06	15.	3.01E 06	25.	4.79E 06	26.
		13.199	483.	10.4	-75.5	8.17	9.96E 06	25.	1.50E 07	29.	6.55E 06	20.	4.04E 06	25.	5.79E 06	24.
15	5/26/66	15.252	296.	36.8	-90.8	9.20	1.91E 08	16.	2.70E 08	27.	2.37E 08	15.	2.51E 08	21.	2.22E 08	9.
		15.262	292.	38.9	-89.2	9.31	2.23E 08	17.	2.92E 08	23.	2.92E 08	15.	2.86E 08	19.	2.61E 08	9.
		15.279	288.	42.5	-86.3	9.53	2.68E 08	16.	3.26E 08	19.	3.38E 08	15.	3.49E 08	19.	3.11E 08	8.
		15.289	288.	44.6	-84.3	9.67	2.79E 08	16.	3.63E 08	22.	3.48E 08	15.	3.62E 08	19.	3.25E 08	9.
		15.299	290.	46.6	-82.2	9.82	2.73E 08	21.	3.91E 08	31.	3.36E 08	19.	3.41E 08	21.	3.15E 08	11.
18	5/27/66	1.125	539.	64.5	-164.6	14.15	3.47E 06	14.	5.11E 06	15.	3.31E 06	42.	3.12E 06	68.	3.83E 06	11.
		1.135	566.	64.2	-159.3	14.51	3.43E 06	13.	3.06E 06	15.	2.64E 06	47.	1.91E 06	88.	3.17E 06	10.
		1.145	595.	63.6	-154.2	14.86	0.0	0.	3.59E 06	16.	0.0	0.	2.16E 06	67.	3.39E 06	16.
20	5/27/66	2.696	594.	1.6	-283.9	7.77	4.05E 06	15.	3.66E 06	18.	1.24E 06	70.	0.0	0.	3.34E 06	23.
		2.706	565.	3.8	-283.1	7.83	4.89E 06	16.	5.97E 06	20.	2.52E 06	30.	6.43E 05	147.	3.37E 06	32.
		2.716	536.	5.9	-282.2	7.90	4.88E 06	20.	9.53E 06	25.	3.91E 06	21.	1.79E 06	45.	3.62E 06	28.
		2.733	492.	9.5	-280.7	8.02	1.20E 07	16.	6.40E 07	74.	5.81E 06	17.	3.84E 06	34.	6.06E 06	26.
		2.743	467.	11.7	-279.8	8.09	1.39E 07	15.	0.0	0.	6.80E 06	16.	5.13E 06	39.	7.91E 06	27.
		2.753	444.	13.9	-278.8	8.16	2.07E 07	22.	0.0	0.	7.71E 06	20.	7.18E 06	48.	8.83E 06	30.
25	5/27/66	10.670	309.	52.7	-7.0	10.20	1.16E 08	16.	1.39E 08	23.	1.35E 08	15.	1.31E 08	20.	1.28E 08	9.
		10.680	318.	54.4	-4.0	10.41	8.67E 07	16.	1.04E 08	23.	1.01E 08	15.	9.53E 07	19.	9.50E 07	9.
		10.690	330.	56.1	-0.8	10.64	6.56E 07	17.	7.96E 07	23.	7.50E 07	16.	6.94E 07	19.	7.09E 07	9.
		10.707	352.	58.7	5.2	11.05	3.92E 07	16.	4.27E 07	19.	4.18E 07	16.	3.81E 07	21.	4.04E 07	9.
		10.717	368.	60.1	9.2	11.33	2.76E 07	16.	3.04E 07	21.	2.89E 07	16.	2.69E 07	22.	2.83E 07	9.
		10.727	385.	61.3	13.6	11.63	1.80E 07	20.	1.89E 07	18.	1.97E 07	21.	1.72E 07	22.	1.84E 07	10.
28	5/27/66	14.439	311.	32.2	-85.1	8.77	8.17E 07	11.	0.0	0.	7.35E 07	15.	8.99E 07	40.	7.90E 07	9.
		14.449	303.	34.4	-83.6	8.87	9.77E 07	13.	0.0	0.	9.76E 07	15.	1.19E 08	35.	9.88E 07	9.
		14.459	297.	36.5	-82.1	8.98	1.19E 08	15.	4.08E 08	70.	1.26E 08	16.	1.47E 08	31.	1.24E 08	10.
		14.475	290.	40.1	-79.4	9.18	1.42E 08	16.	2.69E 08	46.	1.62E 08	15.	1.77E 08	25.	1.56E 08	10.
		14.485	288.	42.3	-77.6	9.31	1.57E 08	16.	3.10E 08	46.	1.79E 08	15.	1.94E 08	24.	1.73E 08	10.
		14.495	288.	44.3	-75.7	9.45	1.59E 08	21.	2.33E 08	36.	1.97E 08	19.	1.92E 08	24.	1.80E 08	12.
33	5/27/66	22.025	623.	-0.6	142.6	7.53	0.0	0.	5.92E 05	15.	0.0	0.	0.0	0.	5.92E 05	15.
		22.035	593.	1.6	143.4	7.60	5.94E 05	13.	7.55E 05	15.	0.0	0.	0.0	0.	6.49E 05	12.
		22.045	563.	3.7	-183.9	7.66	7.05E 05	17.	1.05E 06	15.	0.0	0.	0.0	0.	8.32E 05	20.

PRECEDING PAGE BLANK NOT FILMED.

Table Ic (Continued) NITROGEN DENSITY(NUM/CM3)

TU	DATE	UT (HRS)	ALT (KM)	LAT (DEG)	LONG (DEG)	LT (HRS)	MS1 DEN 1A PEAK	ERR (%)	MS1 DEN 2A PEAK	ERR (%)	MS2 DEN 1A PEAK	ERR (%)	MS2 DEN 2A PEAK	ERR (%)	AVG DEN	ERR (%)
39	5/28/66	13.725	296.	48.9	-51.8	9.61	1.04E 08	16.	1.50E 08	32.	1.21E 08	15.	1.16E 08	20.	1.19E 08	9.
		13.735	302.	50.9	-59.3	9.78	9.05E 07	16.	1.28E 08	32.	1.00E 08	15.	9.81E 07	20.	9.78E 07	9.
		13.745	310.	52.7	-56.8	9.97	7.53E 07	17.	1.08E 08	32.	8.27E 07	16.	8.27E 07	22.	8.11E 07	10.
		13.762	327.	55.6	-51.3	10.33	4.89E 07	16.	6.01E 07	27.	5.26E 07	15.	4.95E 07	20.	5.13E 07	9.
		13.772	339.	57.2	-48.1	10.57	3.63E 07	17.	4.43E 07	27.	3.87E 07	16.	3.59E 07	22.	3.78E 07	9.
		13.782	354.	58.7	-44.4	10.82	2.65E 07	21.	2.94E 07	24.	2.76E 07	20.	2.49E 07	22.	2.68E 07	11.
42	5/28/66	21.541	394.	61.7	-151.3	11.44	1.15E 07	17.	1.54E 07	29.	1.32E 07	17.	1.28E 07	25.	1.27E 07	10.
		21.551	413.	62.7	-146.7	11.77	1.02E 07	17.	1.13E 07	24.	8.76E 06	18.	7.47E 06	26.	9.20E 06	10.
		21.561	434.	63.5	-141.7	12.12	5.46E 06	17.	7.85E 06	24.	6.06E 06	20.	4.59E 06	28.	5.66E 06	11.
		21.575	472.	64.4	-132.8	12.72	2.64E 06	17.	3.59E 06	19.	3.53E 06	23.	2.27E 06	39.	2.93E 06	11.
		21.588	496.	64.6	-127.3	13.10	1.87E 06	16.	2.60E 06	19.	2.42E 06	25.	1.63E 06	48.	2.13E 06	12.
		21.598	522.	64.6	-121.9	13.47	1.89E 06	22.	2.13E 06	19.	2.29E 06	37.	1.21E 06	61.	1.94E 06	13.
46	5/29/66	1.496	609.	63.5	-164.4	14.53	0.0	0.	1.23E 06	16.	0.0	0.	0.0	0.	1.23E 06	16.
47	5/29/66	6.909	599.	0.8	5.7	7.29	5.16E 05	15.	4.16E 05	17.	0.0	0.	0.0	0.	4.61E 05	12.
		6.919	570.	3.0	6.6	7.36	2.32E 05	21.	6.05E 05	15.	0.0	0.	0.0	0.	3.14E 05	49.
		6.929	541.	5.1	7.4	7.42	5.01E 05	15.	7.30E 05	15.	0.0	0.	4.43E 05	168.	5.72E 05	13.
		6.946	496.	8.7	8.9	7.54	5.65E 05	15.	1.27E 06	16.	7.17E 05	56.	7.46E 05	79.	6.74E 05	21.
		6.956	471.	10.9	-350.2	7.61	1.03E 06	23.	1.68E 06	16.	1.09E 06	39.	9.50E 05	56.	1.24E 06	14.
		6.966	448.	13.1	-349.2	7.68	1.27E 06	21.	2.23E 06	17.	1.66E 06	35.	1.25E 06	42.	1.35E 06	15.
48	5/29/66	9.052	291.	46.4	2.6	9.24	9.81E 07	16.	1.83E 08	46.	1.14E 08	15.	1.17E 08	23.	1.09E 08	10.
		9.062	295.	48.4	5.0	9.40	9.97E 07	16.	2.27E 08	57.	1.06E 08	16.	1.13E 08	24.	1.06E 08	10.
		9.079	306.	51.6	9.2	9.69	8.00E 07	16.	1.43E 08	47.	8.31E 07	16.	8.77E 07	26.	8.34E 07	10.
		9.089	314.	53.5	12.0	9.89	5.95E 07	16.	1.10E 08	46.	6.54E 07	16.	6.72E 07	24.	6.38E 07	10.
		9.099	325.	55.2	15.1	10.11	4.51E 07	21.	8.34E 07	52.	4.87E 07	20.	4.92E 07	27.	4.80E 07	13.
57	5/30/66	11.912	612.	-0.3	-73.6	7.00	2.70E 05	16.	4.09E 05	14.	0.0	0.	0.0	0.	3.19E 05	21.
		11.922	581.	1.9	-72.8	7.07	2.60E 05	18.	5.66E 05	15.	0.0	0.	0.0	0.	3.33E 05	39.
		11.932	552.	4.0	-71.9	7.14	4.92E 05	19.	7.66E 05	15.	0.0	0.	0.0	0.	6.00E 05	22.
59	5/30/66	13.975	328.	28.0	-90.2	7.96	2.72E 07	16.	3.34E 07	28.	0.0	0.	0.0	0.	2.83E 07	14.
		13.985	317.	30.2	-88.9	8.05	4.19E 07	17.	5.03E 07	26.	0.0	0.	0.0	0.	4.37E 07	14.
		13.995	308.	32.4	-87.5	8.16	5.57E 07	17.	7.97E 07	32.	0.0	0.	0.0	0.	6.25E 07	15.
		14.011	296.	36.1	-85.1	8.34	9.35E 07	16.	1.41E 08	38.	0.0	0.	0.0	0.	9.71E 07	15.
		14.021	292.	38.2	-83.5	8.45	1.06E 08	16.	1.64E 08	36.	0.0	0.	0.0	0.	1.10E 08	15.
		14.031	289.	40.4	-81.8	8.58	1.10E 08	21.	1.71E 08	43.	0.0	0.	0.0	0.	1.16E 08	19.
68	5/31/66	9.425	306.	51.5	-2.4	9.26	1.53E 08	12.	0.0	0.	0.0	0.	0.0	0.	1.53E 08	12.
		9.435	315.	53.4	0.4	9.46	1.26E 08	14.	3.67E 08	58.	0.0	0.	0.0	0.	1.27E 08	14.
		9.445	326.	55.1	3.4	9.67	9.55E 07	16.	2.12E 08	57.	0.0	0.	0.0	0.	9.73E 07	16.
		9.462	348.	57.9	9.1	10.07	5.81E 07	14.	2.99E 06	84.	0.0	0.	0.0	0.	5.83E 07	14.
		9.472	363.	59.2	13.0	10.34	3.79E 07	15.	8.61E 07	54.	0.0	0.	0.0	0.	3.85E 07	15.
		9.482	379.	60.5	17.1	10.62	2.57E 07	20.	5.13E 07	72.	0.0	0.	0.0	0.	2.61E 07	19.
73	5/31/66	21.091	391.	61.3	-155.8	10.70	4.30E 07	15.	4.43E 07	19.	0.0	0.	0.0	0.	4.35E 07	12.
		21.101	410.	62.3	-151.2	11.02	2.99E 07	15.	2.92E 07	16.	0.0	0.	0.0	0.	2.96E 07	11.
		21.111	431.	63.2	-146.3	11.36	1.79E 07	16.	1.72E 07	17.	0.0	0.	0.0	0.	1.76E 07	12.
		21.128	469.	64.2	-137.5	11.96	1.04E 07	16.	1.07E 07	24.	0.0	0.	0.0	0.	1.05E 07	13.
		21.138	493.	64.5	-132.1	12.33	6.68E 06	16.	8.11E 06	24.	0.0	0.	0.0	0.	7.02E 06	13.
		21.148	519.	64.7	-126.6	12.71	5.29E 06	21.	1.09E 07	40.	0.0	0.	0.0	0.	5.63E 06	24.

Table Id ATOMIC OXYGEN DENSITY(NUM/CM3)

TO	DATE	UT (HRS)	ALT (KM)	LAT (DEG)	LONG (DEG)	LT (HRS)	MS1 DEN 16 PEAK	ERR (%)	MS1 DEN 32 PEAK	ERR (%)	MS2 DEN 16 PEAK	ERR (%)	MS2 DEN 32 PEAK	ERR (%)	AVG DEN	ERR (%)
11	5/26/66	7.377	537.	6.1	-349.5	8.07	8.86E 05	19.	1.67E 05	15.	1.76E 06	75.	0.0	0.	1.09E 06	16.
		7.387	510.	8.2	-348.6	8.14	9.43E 05	16.	2.47E 05	15.	1.77E 06	49.	5.17E 05	167.	1.21E 06	13.
		7.397	484.	10.4	-347.7	8.21	1.16E 06	18.	3.74E 05	15.	2.03E 06	37.	1.28E 06	53.	1.61E 06	22.
		7.413	444.	14.1	-346.2	8.34	1.73E 06	22.	9.27E 05	14.	3.00E 06	26.	4.14E 06	22.	3.12E 06	44.
		7.423	422.	16.3	-345.2	8.41	1.98E 06	26.	1.76E 06	16.	3.93E 06	22.	7.48E 06	24.	4.35E 06	48.
		7.433	402.	18.5	-344.2	8.49	2.03E 06	28.	3.81E 06	27.	4.83E 06	21.	1.32E 07	30.	6.82E 06	49.
14	5/26/66	13.164	579.	2.3	-78.6	7.92	8.57E 05	16.	1.20E 05	15.	0.0	0.	0.0	0.	9.78E 05	14.
		13.180	532.	6.4	-77.2	8.03	1.13E 06	21.	2.84E 05	15.	1.82E 06	45.	1.02E 06	62.	1.48E 06	21.
		13.190	505.	8.5	-76.3	8.10	1.39E 06	21.	4.32E 05	14.	2.47E 06	31.	1.92E 06	34.	2.03E 06	35.
		13.200	480.	10.7	-75.4	8.17	1.46E 06	24.	8.16E 05	14.	3.09E 06	28.	3.49E 06	26.	2.62E 06	48.
15	5/26/66	15.233	296.	37.1	-90.6	9.21	1.79E 07	22.	3.91E 07	12.	1.38E 07	19.	9.89E 07	21.	6.10E 07	23.
		15.263	291.	39.2	-89.3	9.33	1.91E 07	20.	4.26E 07	12.	1.29E 07	19.	1.04E 08	20.	6.62E 07	22.
		15.280	288.	42.8	-86.0	9.54	1.93E 07	21.	4.71E 07	13.	1.41E 07	18.	1.08E 08	19.	7.26E 07	24.
		15.290	289.	44.8	-84.1	9.69	1.77E 07	22.	4.76E 07	12.	1.32E 07	18.	1.07E 08	20.	7.01E 07	22.
		15.300	291.	46.9	-81.9	9.84	1.69E 07	22.	4.49E 07	12.	1.26E 07	19.	1.01E 08	22.	6.59E 07	20.
18	5/27/66	1.126	542.	64.5	-163.9	14.20	1.82E 06	17.	1.23E 06	14.	2.59E 06	121.	4.83E 06	73.	3.07E 06	11.
		1.136	570.	64.1	-158.6	14.56	1.38E 06	13.	7.43E 05	13.	2.01E 06	108.	3.35E 06	68.	2.14E 06	10.
		1.146	599.	63.6	-153.6	14.91	9.65E 05	16.	4.48E 05	14.	2.40E 06	81.	2.47E 06	76.	1.42E 06	15.
20	5/27/66	2.697	590.	1.9	-283.8	7.78	8.11E 05	24.	1.87E 05	15.	0.0	0.	0.0	0.	9.98E 05	19.
		2.707	561.	4.0	-283.0	7.84	9.27E 05	21.	3.12E 05	14.	0.0	0.	0.0	0.	1.24E 06	16.
		2.717	533.	6.2	-282.1	7.91	9.90E 05	26.	6.06E 05	13.	0.0	0.	1.45E 06	67.	1.60E 06	17.
		2.734	489.	9.8	-280.6	8.03	8.52E 05	33.	2.50E 06	33.	2.42E 06	41.	4.51E 06	33.	4.04E 06	35.
		2.744	464.	12.0	-279.7	8.10	6.32E 05	36.	6.21E 06	50.	3.23E 06	30.	7.48E 06	39.	8.89E 06	25.
		2.754	441.	14.2	-278.7	8.17	1.35E 06	38.	0.0	0.	4.01E 06	27.	1.34E 07	52.	1.74E 07	40.
25	5/27/66	10.671	310.	52.9	-6.6	10.23	1.39E 07	28.	5.81E 07	11.	9.40E 06	30.	1.15E 08	20.	7.70E 07	20.
		10.681	320.	54.7	-3.6	10.44	1.23E 07	22.	4.50E 07	13.	7.34E 06	24.	9.18E 07	19.	6.21E 07	21.
		10.691	331.	56.3	-0.4	10.67	1.13E 07	20.	3.48E 07	13.	6.28E 06	24.	8.03E 07	20.	4.95E 07	23.
		10.708	354.	58.9	5.7	11.09	7.54E 06	23.	2.08E 07	13.	4.61E 06	29.	5.46E 07	22.	3.04E 07	25.
		10.718	370.	60.2	9.8	11.37	6.24E 06	20.	1.44E 07	12.	3.92E 06	30.	4.08E 07	21.	2.20E 07	26.
		10.728	387.	61.4	14.2	11.67	4.66E 06	20.	9.85E 06	13.	3.21E 06	35.	2.98E 07	22.	1.55E 07	27.
28	5/27/66	14.440	310.	32.5	-84.9	8.78	0.0	0.	2.60E 08	79.	1.32E 07	28.	1.28E 08	40.	1.40E 08	37.
		14.460	296.	36.8	-81.9	9.00	5.65E 06	31.	1.16E 08	32.	1.40E 07	20.	0.0	0.	1.22E 08	30.
		14.477	289.	40.4	-79.2	9.20	1.04E 07	29.	1.04E 08	21.	1.53E 07	21.	1.54E 08	23.	1.29E 08	17.
		14.487	288.	42.3	-77.4	9.33	1.25E 07	26.	9.77E 07	17.	1.55E 07	19.	1.58E 08	23.	1.21E 08	19.
		14.497	289.	44.6	-75.4	9.47	1.38E 07	25.	9.11E 07	16.	1.50E 07	19.	1.50E 08	23.	1.19E 08	18.
33	5/27/66	22.037	589.	1.8	143.5	7.61	3.62E 05	14.	1.09E 05	14.	0.0	0.	0.0	0.	4.71E 05	11.
		22.047	560.	4.0	-215.6	7.67	4.89E 05	14.	1.82E 05	14.	0.0	0.	5.64E 05	102.	4.71E 05	11.

Table Id (Continued) ATOMIC OXYGEN DENSITY(NUM/CM3)

TD	DATE	UT (HRS)	ALT (KM)	LAT (DEG)	LONG (DEG)	LT (HRS)	MS1 DEN 16 PEAK	ERR (%)	MS1 DEN 32 PEAK	ERR (%)	MS2 DEN 16 PEAK	ERR (%)	MS2 DEN 32 PEAK	ERR (%)	AVG DEN	ERR (%)
39	5/28/66	13.727	297.	49.2	-61.5	9.63	1.19E 07	30.	9.23E 07	15.	1.42E 07	26.	1.48E 08	20.	1.14E 08	19.
		13.737	303.	51.1	-58.9	9.81	8.99E 06	25.	8.27E 07	14.	1.03E 07	22.	1.27E 08	21.	9.96E 07	17.
		13.747	311.	52.9	-56.2	10.00	8.20E 06	23.	6.91E 07	15.	7.58E 06	23.	1.09E 08	20.	8.42E 07	17.
		13.763	329.	55.8	-51.1	10.36	6.76E 06	25.	4.38E 07	12.	5.48E 06	26.	8.19E 07	21.	5.41E 07	20.
		13.773	341.	57.4	-47.6	10.60	5.76E 06	23.	3.26E 07	12.	4.54E 06	26.	6.83E 07	21.	4.08E 07	21.
		13.783	356.	58.9	-43.9	10.86	5.08E 06	22.	2.37E 07	12.	3.78E 06	30.	5.18E 07	22.	3.09E 07	22.
42	5/28/66	21.543	396.	61.8	-150.8	11.49	2.59E 06	28.	1.22E 07	11.	2.91E 06	79.	2.04E 07	24.	1.59E 07	22.
		21.553	416.	62.8	-146.0	11.82	2.09E 06	22.	7.50E 06	13.	1.98E 06	74.	1.87E 07	23.	1.01E 07	24.
		21.563	437.	63.6	-141.0	12.16	1.60E 06	21.	4.79E 06	13.	1.08E 06	77.	1.24E 07	23.	6.74E 06	24.
		21.579	475.	64.4	-132.1	12.77	1.15E 06	20.	2.24E 06	14.	1.31E 06	96.	6.82E 06	25.	3.54E 06	23.
		21.589	500.	64.6	-126.6	13.15	7.85E 05	20.	1.47E 06	14.	1.21E 06	92.	4.87E 06	28.	2.33E 06	23.
		21.599	526.	64.6	-121.1	13.52	6.79E 05	18.	9.10E 05	14.	1.06E 06	110.	3.57E 06	32.	1.62E 06	20.
47	5/29/66	6.910	595.	1.1	5.8	7.30	3.54E 05	22.	1.66E 05	19.	0.0	0.	1.29E 06	168.	5.20E 05	16.
		6.920	566.	3.2	6.7	7.37	2.69E 05	19.	1.75E 05	16.	0.0	0.	1.05E 06	122.	4.44E 05	13.
		6.930	537.	5.4	7.6	7.43	3.94E 05	16.	2.76E 05	14.	0.0	0.	1.20E 06	82.	6.69E 05	11.
		6.947	493.	9.0	9.0	7.55	6.03E 05	17.	6.56E 05	14.	0.0	0.	2.08E 06	38.	1.26E 06	11.
		6.957	468.	11.2	-350.0	7.62	8.68E 05	16.	1.05E 06	14.	7.76E 05	98.	3.15E 06	26.	1.90E 06	18.
		6.967	445.	13.4	-349.1	7.69	1.04E 06	17.	1.75E 06	14.	9.15E 05	84.	4.86E 06	21.	2.98E 06	23.
48	5/29/66	9.054	291.	46.7	3.0	9.26	7.31E 06	27.	1.17E 08	17.	1.56E 07	20.	1.60E 08	21.	1.23E 08	16.
		9.064	296.	48.7	5.3	9.42	5.03E 06	28.	1.17E 08	21.	1.31E 07	20.	1.51E 08	23.	1.35E 08	19.
		9.080	307.	51.9	9.6	9.72	3.36E 06	30.	9.90E 07	25.	8.55E 06	23.	1.19E 08	23.	1.13E 08	16.
		9.090	316.	53.7	12.4	9.92	3.44E 06	28.	8.11E 07	27.	6.99E 06	22.	9.86E 07	23.	9.46E 07	17.
		9.100	326.	55.4	15.5	10.14	3.28E 06	28.	5.71E 07	22.	5.64E 06	24.	8.90E 07	26.	6.91E 07	21.
57	5/30/66	11.924	578.	2.1	-72.7	7.08	3.62E 05	15.	1.41E 05	15.	0.0	0.	0.0	0.	5.03E 05	12.
		11.934	549.	4.3	-71.8	7.15	5.05E 05	15.	2.48E 05	14.	0.0	0.	0.0	0.	7.54E 05	11.
59	5/30/66	13.976	327.	28.3	-90.0	7.98	4.16E 06	30.	3.64E 07	12.	0.0	0.	0.0	0.	4.06E 07	12.
		13.986	316.	30.5	-88.7	8.07	4.37E 06	25.	4.68E 07	15.	0.0	0.	0.0	0.	5.12E 07	13.
		13.996	307.	32.7	-87.3	8.17	5.02E 06	25.	5.70E 07	15.	0.0	0.	0.0	0.	6.20E 07	14.
		14.013	295.	36.4	-84.9	8.35	5.45E 06	28.	8.21E 07	17.	0.0	0.	0.0	0.	8.74E 07	16.
		14.023	291.	38.5	-83.3	8.47	5.78E 06	27.	9.18E 07	17.	0.0	0.	0.0	0.	9.78E 07	16.
		14.033	289.	40.7	-81.6	8.59	5.66E 06	28.	9.54E 07	19.	0.0	0.	0.0	0.	1.02E 08	18.
68	5/31/66	9.427	308.	51.8	-2.1	9.29	1.67E 06	50.	1.42E 08	31.	0.0	0.	0.0	0.	1.44E 08	30.
		9.437	317.	53.6	0.8	9.49	1.52E 06	36.	1.26E 08	31.	0.0	0.	0.0	0.	1.28E 08	30.
		9.447	328.	55.3	3.9	9.70	1.26E 06	35.	1.00E 08	31.	0.0	0.	0.0	0.	1.02E 08	31.
		9.463	350.	58.0	9.6	10.10	9.10E 05	37.	6.18E 07	33.	0.0	0.	0.0	0.	6.27E 07	32.
		9.473	365.	59.4	13.5	10.37	1.30E 06	30.	3.95E 07	26.	0.0	0.	0.0	0.	4.07E 07	26.
		9.483	382.	60.7	17.6	10.66	1.11E 06	29.	3.14E 07	33.	0.0	0.	0.0	0.	3.25E 07	31.
73	5/31/66	21.093	394.	61.4	-155.2	10.75	3.09E 06	24.	1.65E 07	13.	0.0	0.	0.0	0.	1.98E 07	11.
		21.103	413.	62.4	-150.5	11.07	2.58E 06	18.	1.29E 07	13.	0.0	0.	0.0	0.	1.55E 07	11.
		21.113	434.	63.3	-145.6	11.41	2.13E 06	18.	9.39E 06	13.	0.0	0.	0.0	0.	1.15E 07	11.
		21.129	472.	64.3	-136.8	12.01	1.71E 06	21.	6.27E 06	11.	0.0	0.	0.0	0.	7.99E 06	10.
		21.139	496.	64.6	-131.4	12.38	1.17E 06	22.	4.59E 06	11.	0.0	0.	0.0	0.	5.78E 06	10.
		21.149	522.	64.7	-125.9	12.76	9.46E 05	25.	4.45E 06	18.	0.0	0.	0.0	0.	5.40E 06	15.

Table II NUMBER DENSITIES (NUM/CM3)

TP	DATE	UT (HRS)	ALT (KM)	LAT (DEG)	LONG (DEG)	LT (HRS)	ATOMIC HYDROGEN	ATOMIC HELIUM	MOLEC NITROGEN	ATOMIC OXYGEN	MASS DENSITY	MEAN MASS	CP
8	5/26/66	7.375	540.	5.8	-349.7	9.1	1.69E 05	1.03E 06	3.64E 05	1.03E 06	2.09E-14	17.2	3.57E-03
		7.385	513.	7.9	-349.8	8.1	2.04E 06	1.12E 06	4.00E 05	1.19E 05	2.31E-14	16.7	3.64E-03
		7.395	487.	10.1	-347.9	8.2	2.20E 06	1.16E 06	3.93E 06	1.55E 06	2.38E-14	16.2	4.05E-03
		7.412	447.	13.9	-346.3	8.3	2.96E 06	1.33E 06	5.41E 06	2.96E 06	3.48E-14	16.6	7.52E-03
		7.422	428.	16.0	-345.3	8.4	3.70E 06	1.41E 06	7.79E 06	4.16E 05	4.03E-14	17.5	8.98E-03
		7.432	404.	18.2	-344.3	8.5	4.94E 06	1.43E 06	1.20E 07	6.42E 06	7.55E-14	18.2	1.15E-02
16	5/26/66	15.252	256.	36.8	-90.8	9.2	5.64E 06	7.19E 05	2.22E 08	6.04E 07	1.19E-14	24.9	5.76E-02
		15.262	292.	33.9	-89.2	9.3	4.45E 06	6.23E 05	2.61E 08	6.94E 07	1.39E-14	25.2	7.86E-02
		15.279	289.	42.5	-86.3	9.5	3.92E 06	6.10E 05	3.11E 08	7.20E 07	1.53E-14	25.5	8.15E-02
		15.289	288.	44.6	-84.3	9.7	4.59E 06	5.49E 05	3.25E 08	7.04E 07	1.70E-14	25.6	8.66E-02
		15.299	290.	46.6	-82.2	9.9	7.43E 06	5.54E 05	3.19E 08	6.61E 07	1.66E-14	25.8	8.06E-02
20	5/27/66	2.696	594.	1.6	-283.9	7.8	1.99E 06	1.24E 06	3.34E 05	9.69E 05	1.95E-16	15.6	2.87E-03
		2.706	565.	3.8	-283.1	7.8	2.47E 06	1.40E 06	3.37E 05	1.20E 06	2.07E-14	14.5	2.86E-03
		2.716	536.	5.9	-282.2	7.9	4.29E 06	1.69E 05	3.53E 05	1.54E 06	2.34E-16	12.7	3.48E-03
		2.733	492.	9.5	-280.7	8.0	6.05E 06	1.96E 06	6.06E 05	3.75E 06	4.13E-16	14.1	6.76E-03
		2.743	467.	11.7	-279.8	8.1	7.24E 06	1.94E 06	7.81E 05	7.93E 05	6.09E-16	14.8	1.35E-02
		2.753	444.	13.9	-278.8	8.2	8.26E 06	2.20E 06	9.83E 06	1.59E 07	9.74E-16	15.0	2.51E-02
25	5/27/66	10.670	309.	52.7	-7.0	10.2	2.84E 06	1.52E 06	1.29E 08	7.93E 07	8.04E-15	23.0	5.48E-02
		10.680	318.	54.4	-4.0	10.4	2.39E 06	1.59E 06	9.50E 07	6.39E 07	6.12E-15	22.7	5.08E-02
		10.690	330.	56.1	-0.8	10.5	2.10E 06	1.59E 06	7.03E 07	5.10E 07	4.66E-15	22.4	4.57E-02
		10.707	352.	58.7	5.2	11.1	2.29E 06	1.40E 06	4.04E 07	3.16E 07	2.73E-15	21.7	3.97E-02
		10.717	368.	60.1	9.2	11.3	2.03E 06	1.28E 06	2.83E 07	2.30E 07	1.94E-15	21.4	3.61E-02
		10.727	385.	61.3	13.6	11.6	2.13E 06	1.24E 06	1.98E 07	1.62E 07	1.30E-15	20.2	3.12E-02
28	5/27/66	14.439	318.	32.2	-95.1	9.9	5.69E 06	2.11E 06	7.90E 07	0.0	0.0	0.0	0.0
		14.449	303.	34.4	-93.6	9.9	4.93E 06	2.14E 06	9.88E 07	0.0	0.0	0.0	0.0
		14.459	297.	36.5	-92.1	9.9	3.62E 06	1.99E 06	1.23E 08	0.0	0.0	0.0	0.0
		14.475	290.	40.1	-79.4	9.2	3.46E 06	2.11E 06	1.56E 08	1.29E 08	1.07E-14	22.2	6.55E-02
		14.485	288.	42.3	-77.6	9.1	3.44E 06	1.78E 06	1.73E 08	1.22E 08	1.13E-14	22.7	6.99E-02
		14.495	288.	44.3	-75.7	9.5	3.63E 06	1.71E 06	1.40E 08	1.15E 08	1.14E-14	23.0	6.72E-02
39	5/28/66	13.725	296.	48.9	-61.8	9.6	3.26E 06	1.44E 06	1.15E 08	1.16E 08	8.42E-15	21.4	1.00E-01
		13.735	302.	50.9	-59.3	9.9	3.06E 06	1.41E 06	9.76E 07	1.01E 08	7.22E-15	21.5	9.60E-02
		13.745	310.	52.7	-56.6	10.0	3.50E 06	1.31E 06	8.11E 07	9.60E 07	6.07E-15	21.3	9.42E-02
		13.762	327.	55.5	-51.5	10.3	3.01E 06	1.17E 06	5.13E 07	5.61E 07	3.98E-15	21.0	8.11E-02
		13.772	339.	57.2	-48.1	10.5	2.66E 06	1.36E 06	3.78E 07	4.23E 07	2.90E-15	20.8	6.94E-02
		13.782	354.	58.7	-44.5	10.5	1.88E 06	1.06E 06	2.68E 07	3.17E 07	2.10E-15	20.6	6.52E-02

Table II (Continued) NUMBER DENSITIES (NUM/CM3)

TQ	DATE	UT (HRS)	ALT (KM)	LAT (DEG)	LONG (DEG)	LT (HRS)	ATOMIC HYDROGEN	HELIUM	MOLEC NITROGEN	ATOMIC OXYGEN	MASS DENSITY	MEAN MASS	CD
42	5/28/66	21.241	394.	61.7	-151.5	11.4	2.42E 06	6.50E 05	1.27E 07	1.65E 07	1.04E-15	15.4	7.22E-02
		21.551	413.	62.7	-146.7	11.9	2.27E 06	5.11E 05	9.20E 06	1.07E 07	7.22E-16	15.2	5.70E-02
		21.561	434.	63.5	-141.7	12.1	2.27E 06	5.93E 05	5.44E 06	7.12E 06	4.63E-16	17.5	4.70E-02
		21.578	472.	64.4	-132.8	12.7	1.50E 06	5.17E 05	2.93E 06	3.73E 06	2.43E-16	16.5	3.59E-02
		21.588	496.	64.6	-127.3	13.1	1.09E 06	4.12E 05	2.13E 06	2.45E 06	1.73E-16	15.0	3.23E-02
		21.598	522.	64.6	-121.9	13.5	1.40E 06	2.92E 05	1.94E 06	1.70E 06	1.42E-16	14.0	3.12E-02
47	5/29/66	6.909	599.	0.8	5.7	7.3	1.70E 05	8.93E 05	4.51E 03	5.31E 05	4.18E-17	13.5	5.56E-02
		6.919	570.	3.0	6.6	7.4	3.52E 05	1.00E 06	3.13E 05	4.54E 05	3.50E-17	9.6	4.45E-02
		6.929	541.	5.1	7.4	7.4	3.85E 05	1.30E 06	5.73E 03	6.74E 05	5.32E-17	11.1	4.19E-02
		6.946	496.	8.7	8.9	7.3	6.64E 05	1.20E 06	6.74E 05	1.20E 05	7.37E-17	11.4	4.13E-02
		6.956	471.	10.9	-350.2	7.5	7.90E 05	1.42E 06	1.23E 05	1.87E 06	1.19E-15	13.5	5.08E-02
		6.956	448.	13.1	-349.2	7.7	6.93E 05	1.53E 06	1.55E 06	2.40E 06	1.59E-16	14.5	7.15E-02
48	5/29/66	9.052	591.	46.4	2.6	9.2	3.64E 06	1.44E 06	1.04E 03	0.0	0.0	0.0	0.0
		9.062	299.	48.4	5.0	9.4	3.47E 06	1.69E 06	1.06E 03	1.33E 03	8.67E-15	20.0	1.06E-01
		9.079	306.	51.6	9.2	9.7	3.22E 06	1.50E 06	8.34E 07	1.15E 08	6.33E-15	20.6	1.13E-01
		9.095	314.	53.5	12.0	9.9	3.63E 06	1.38E 06	6.39E 07	9.69E 07	5.55E-15	20.2	1.17E-01
		9.099	325.	55.2	13.1	10.1	3.71E 06	1.33E 06	4.80E 07	7.12E 07	4.14E-15	20.1	9.76E-02
59	5/30/66	13.975	329.	29.0	-30.2	9.0	3.04E 05	1.72E 06	2.83E 07	3.93E 07	2.38E-15	19.8	5.01E-02
		13.985	317.	30.2	-38.9	9.1	2.94E 05	1.59E 06	4.37E 07	4.96E 07	3.36E-15	20.7	5.36E-02
		13.995	309.	32.4	-47.5	9.2	2.92E 06	1.74E 06	5.25E 07	6.04E 07	4.52E-15	21.4	5.70E-02
		14.011	296.	36.1	-65.1	9.3	3.12E 05	1.59E 06	9.71E 07	8.51E 07	6.78E-15	21.9	6.56E-02
		14.021	292.	38.2	-83.5	9.5	4.02E 06	1.63E 06	1.10E 08	9.63E 07	7.69E-15	21.9	7.78E-02
		14.031	289.	40.4	-31.8	9.5	3.93E 06	1.69E 06	1.16E 08	1.01E 08	8.09E-15	21.9	7.58E-02
68	5/31/66	9.425	306.	51.5	-2.4	9.3	5.14E 05	1.27E 05	1.53E 08	1.46E 08	1.10E-14	21.7	1.20E-01
		9.435	315.	53.4	0.4	9.5	4.69E 05	1.13E 06	1.27E 08	1.30E 08	9.37E-15	21.5	1.10E-01
		9.445	325.	55.1	3.4	9.7	0.0	1.07E 06	9.71E 07	1.05E 08	7.30E-15	21.7	1.32E-01
		9.462	348.	57.9	9.1	10.1	0.0	1.22E 06	5.83E 07	6.52E 07	4.44E-15	21.5	9.71E-02
		9.472	363.	59.2	13.0	10.3	6.35E 06	1.01E 06	3.85E 07	4.30E 07	2.95E-15	20.1	9.07E-02
		9.482	379.	60.5	17.1	10.5	3.20E 06	9.23E 05	2.61E 07	3.35E 07	2.11E-15	20.7	8.08E-02
73	5/31/66	21.091	391.	61.3	-155.8	10.7	1.48E 05	3.32E 05	4.35E 07	2.02E 07	2.56E-15	23.6	9.57E-02
		21.101	410.	62.3	-151.2	11.0	1.14E 06	3.50E 05	2.95E 07	1.60E 07	1.80E-15	23.1	8.43E-02
		21.111	431.	63.2	-146.3	11.4	8.98E 05	3.34E 05	1.76E 07	1.20E 07	1.14E-15	23.3	7.70E-02
		21.128	469.	64.2	-137.5	12.0	2.32E 06	2.98E 05	1.05E 07	8.22E 06	7.15E-16	20.2	7.86E-02
		21.138	493.	64.5	-132.1	12.3	2.66E 06	3.12E 05	7.02E 06	6.02E 06	4.96E-16	19.7	6.46E-02

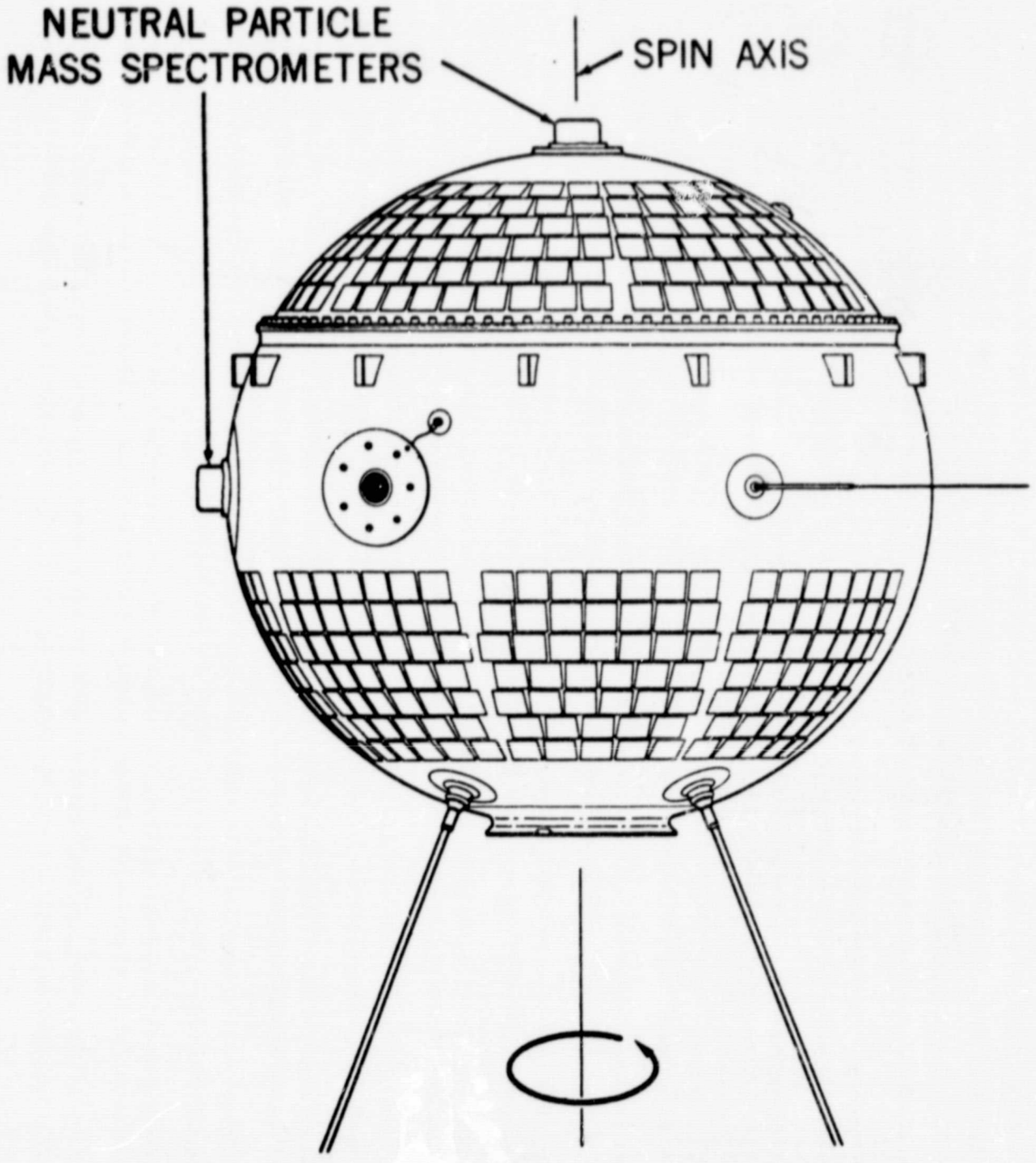

Figure 1. Explorer 32 satellite showing one mass spectrometer located on spin axis (polar) and one mass spectrometer located on spin equator (equatorial).

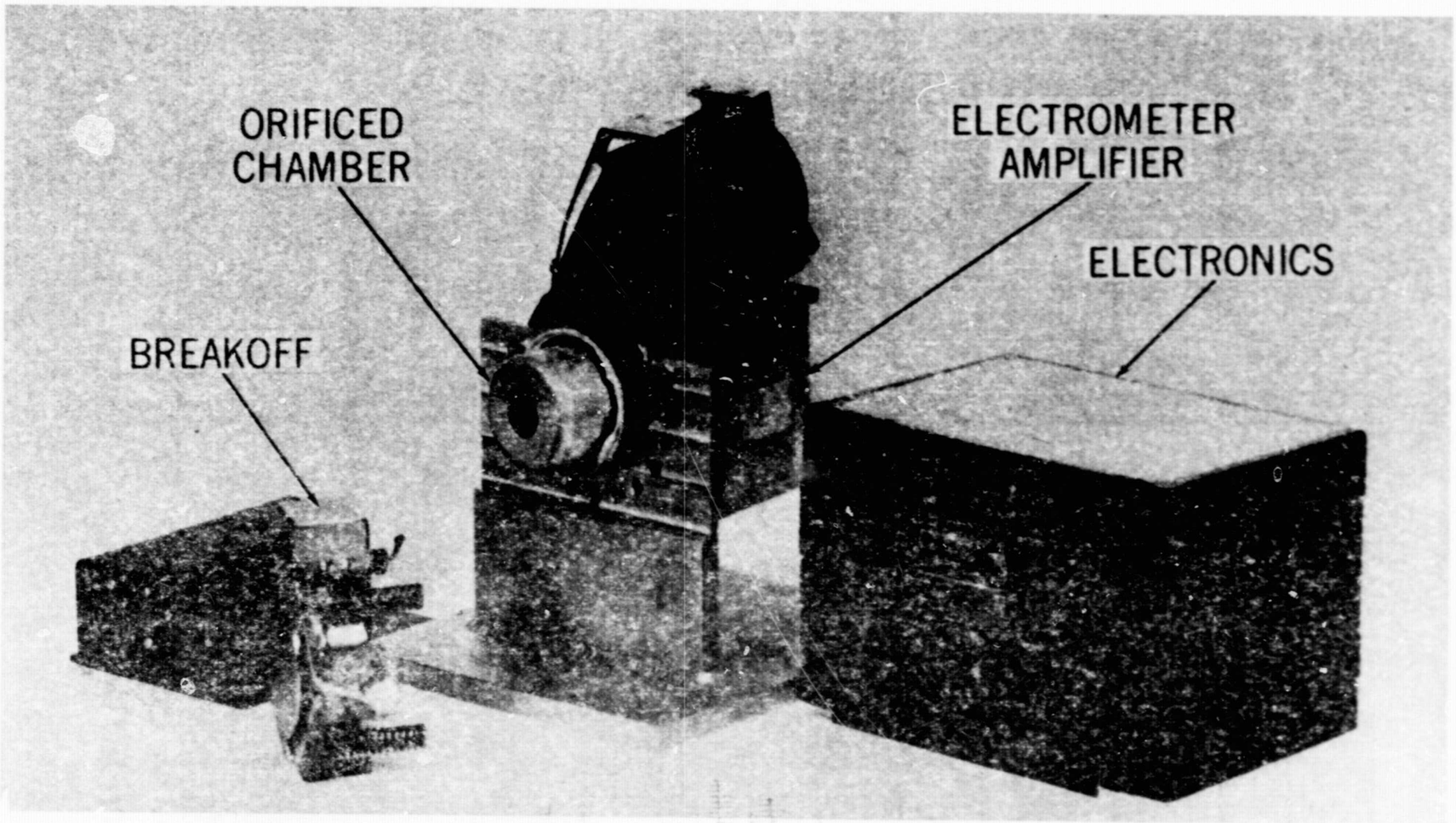

Figure 2. Complete mass spectrometer system.

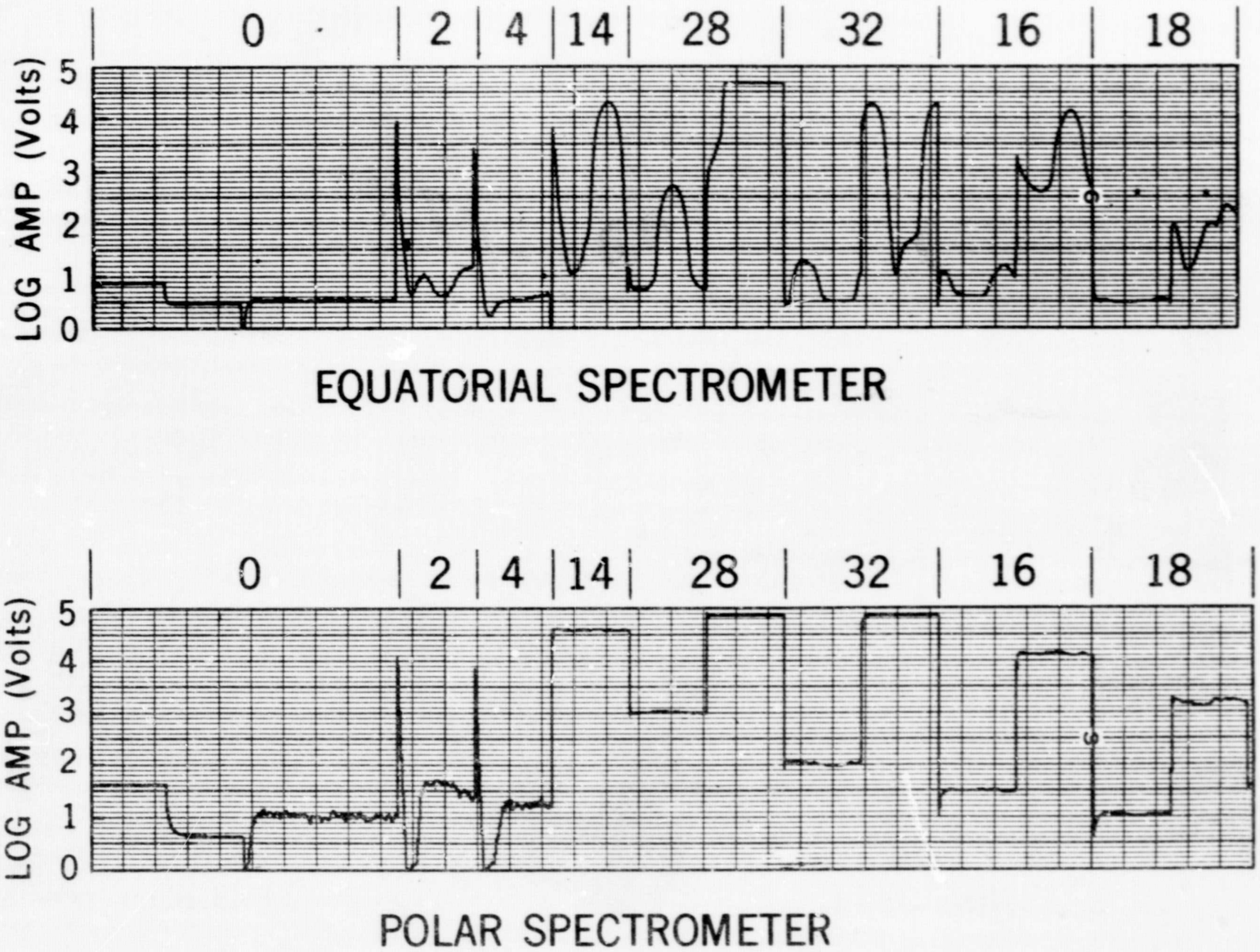

Figure 3. Logarithmic amplifier output for the equatorial and polar mass spectrometers. Note large modulation on equatorial spectrometer output caused by the ram/rarefaction motion of the spinning satellite.

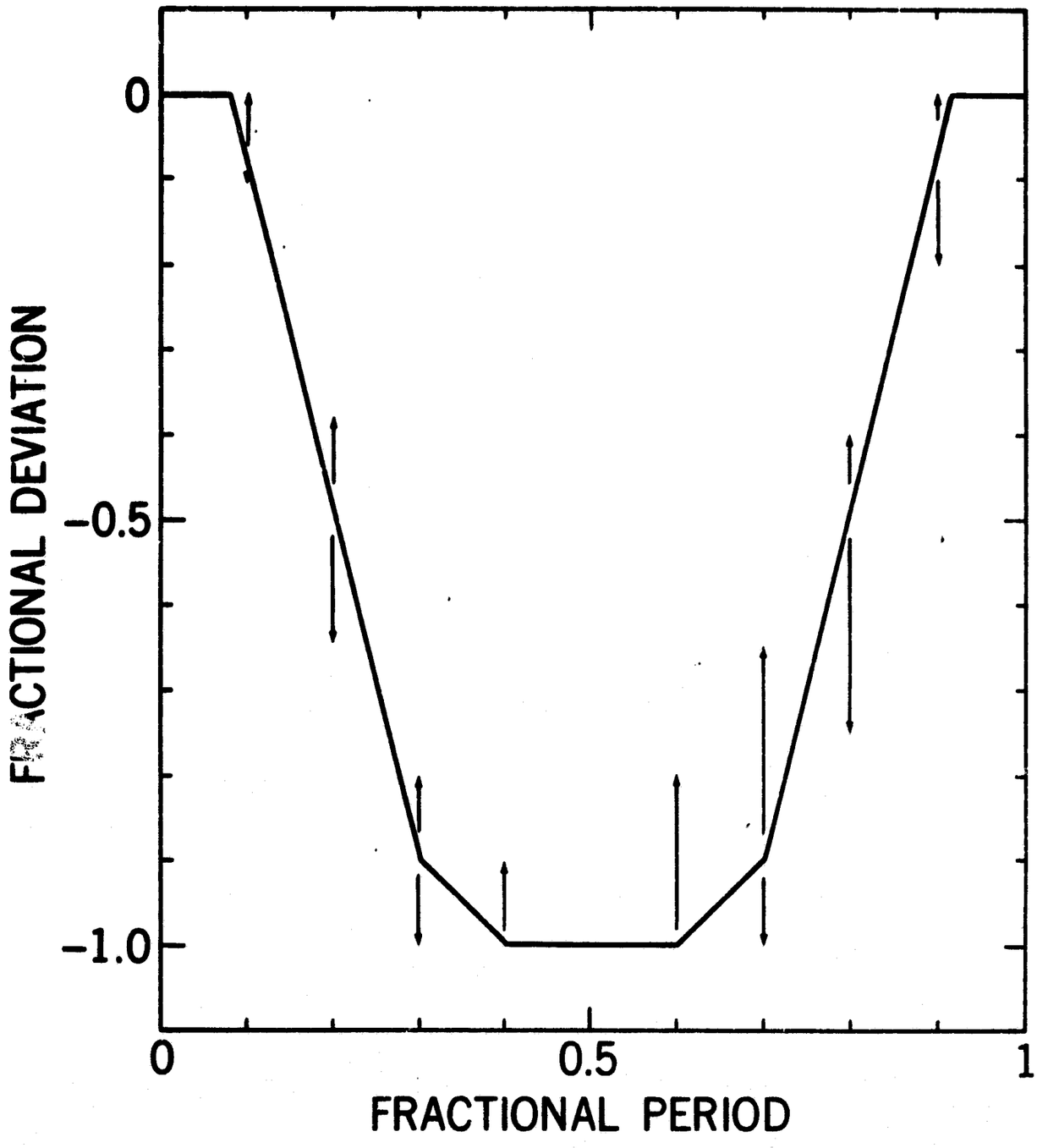

Figure 4. Repeller voltage deviation during a spin cycle. Error bars indicate variability of deviation from one spin cycle to another.

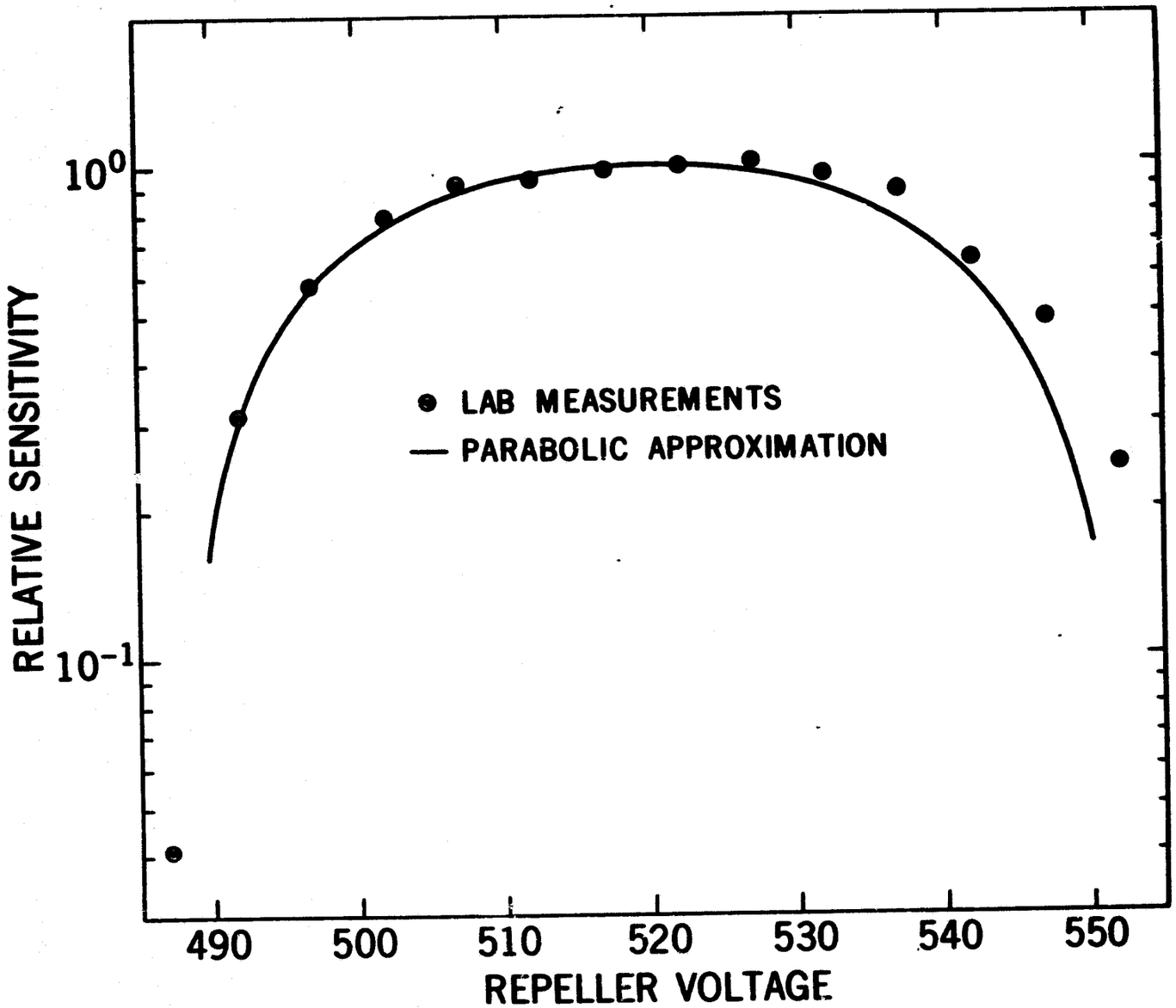

Figure 5. Effect of repeller voltage change on the relative sensitivity of the mass 28 peak. The normal operating voltage was 519 volts. Similar effects were observed for all masses.

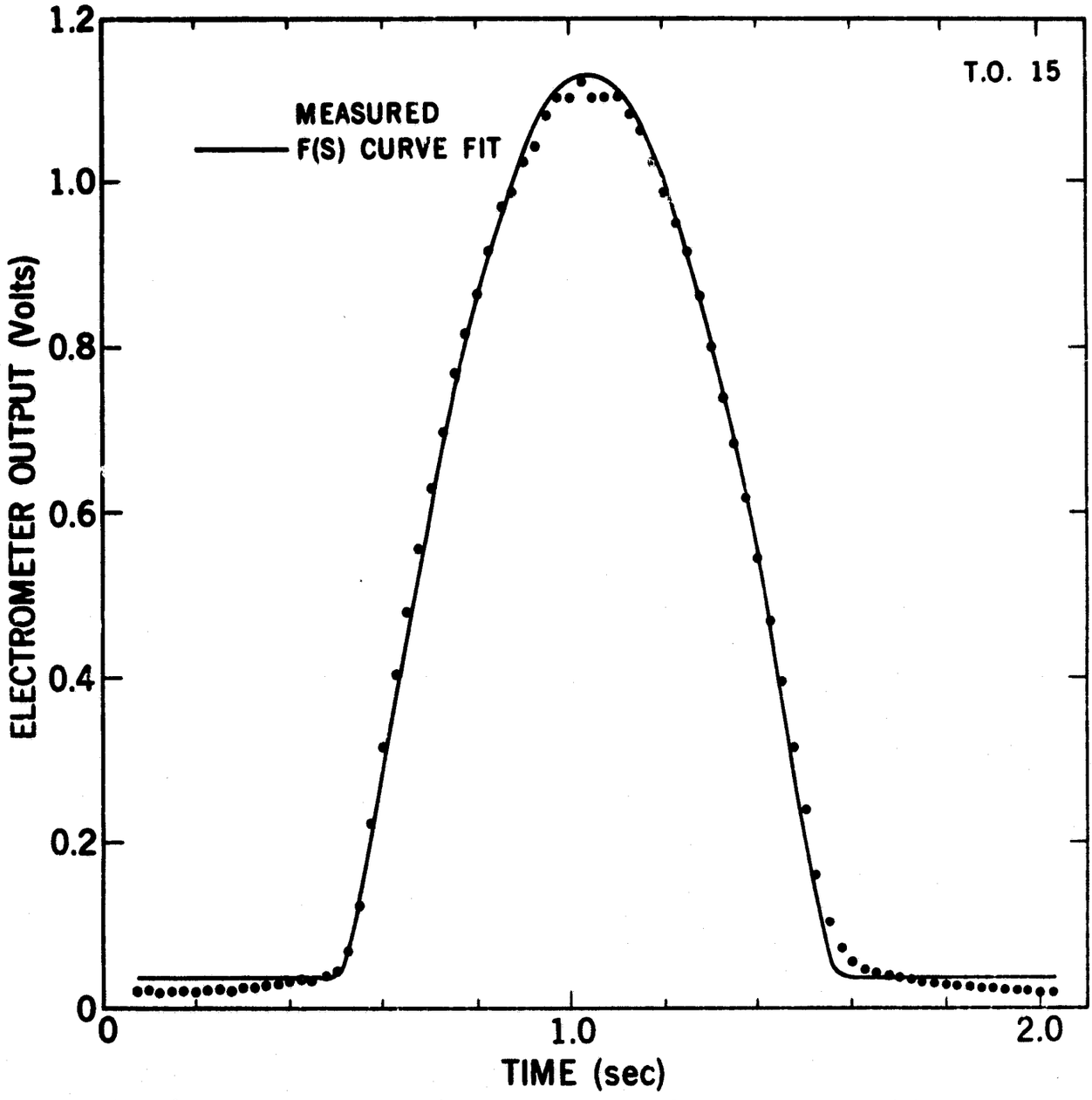

Figure 6. Electrometer output voltage for mass 28 taken near perigee (alt < 400 km). Note satisfactory agreement between measured values and least square F(S) fit.

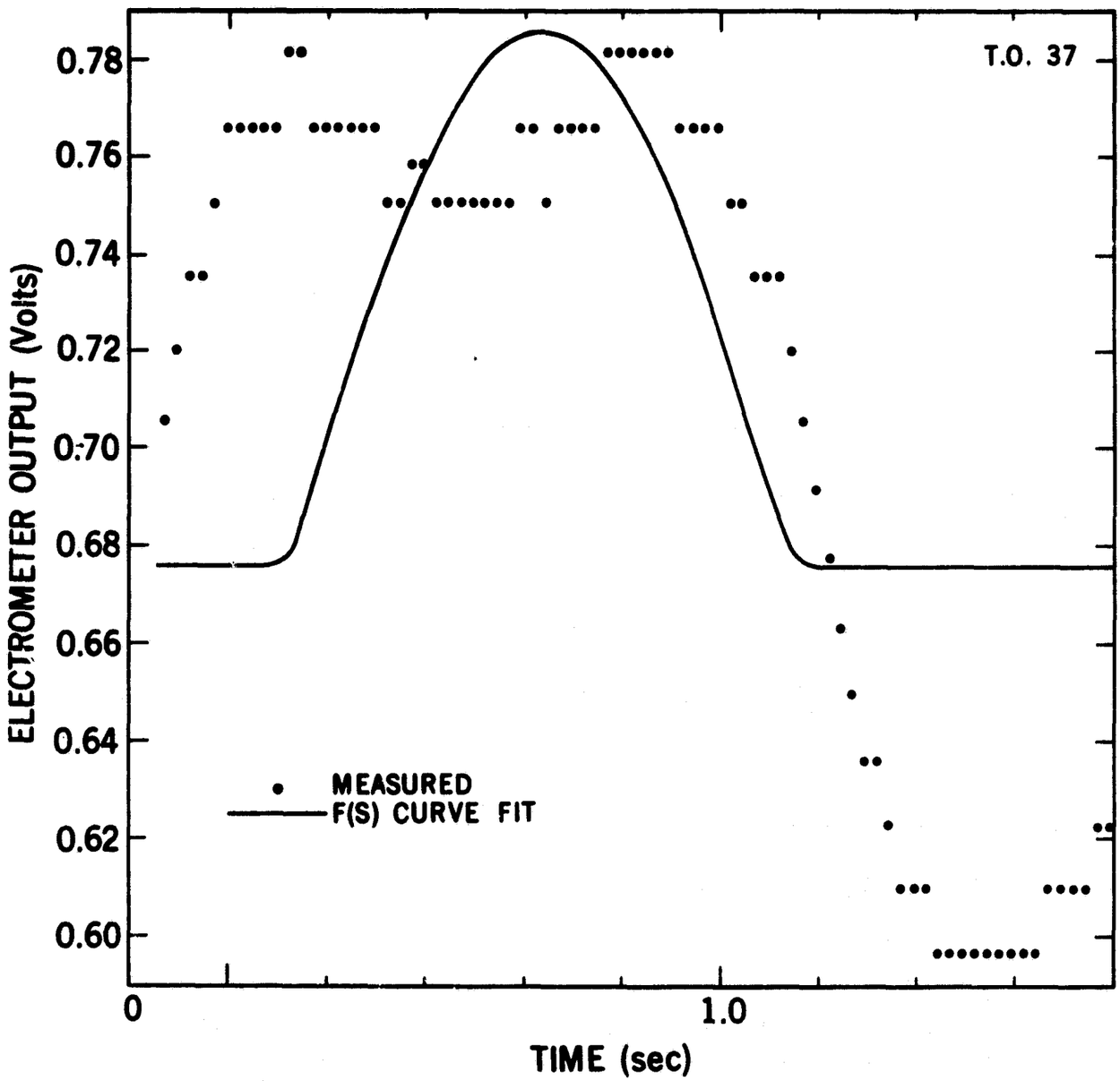

Figure 7. Electrometer output voltage for mass 28 taken at an altitude > 500 km. Note poor agreement between measured values and least square F(S) fit.

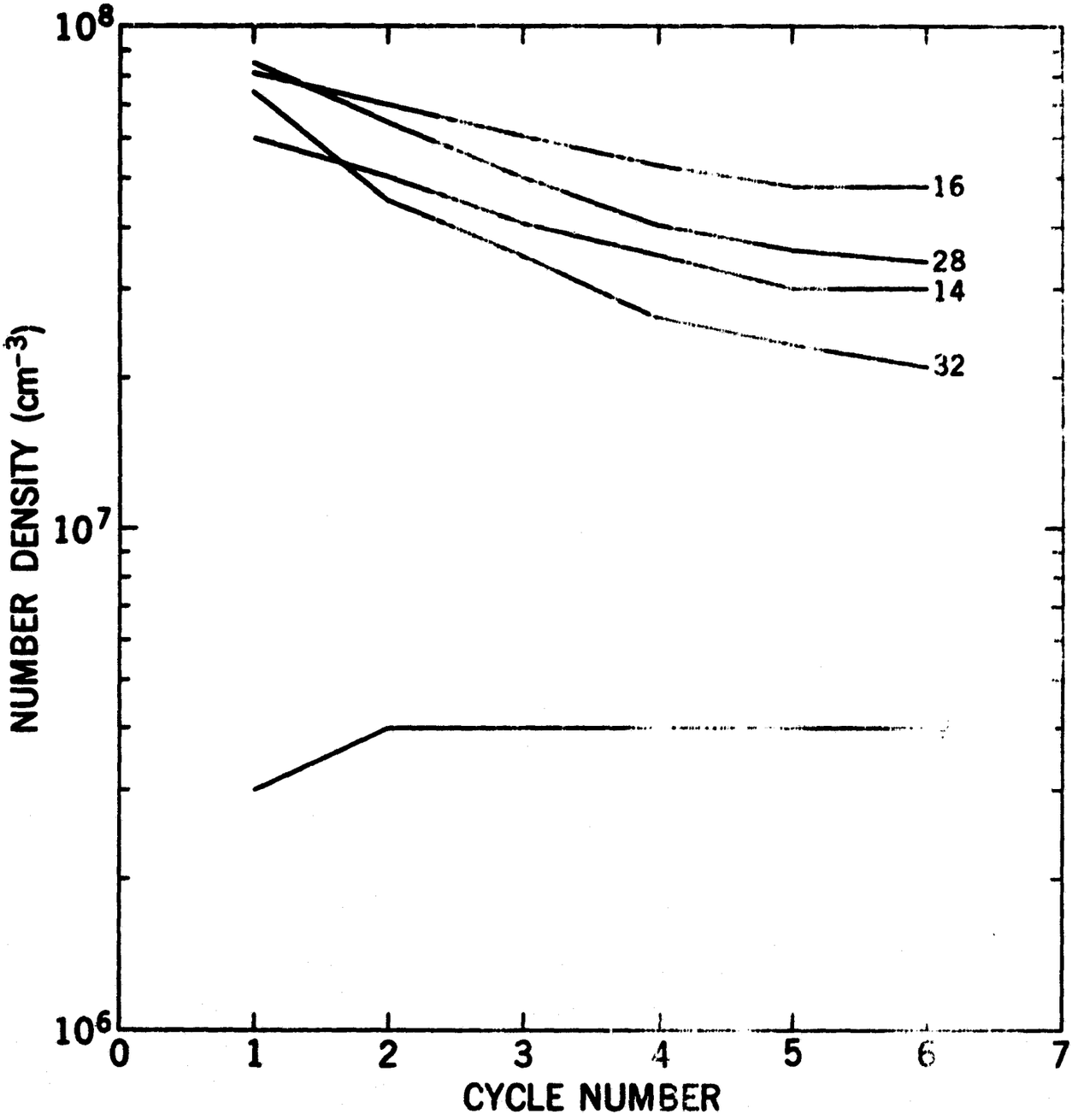

Figure 8. Background densities for polar spectrometer as a function of time from each filament turn on.

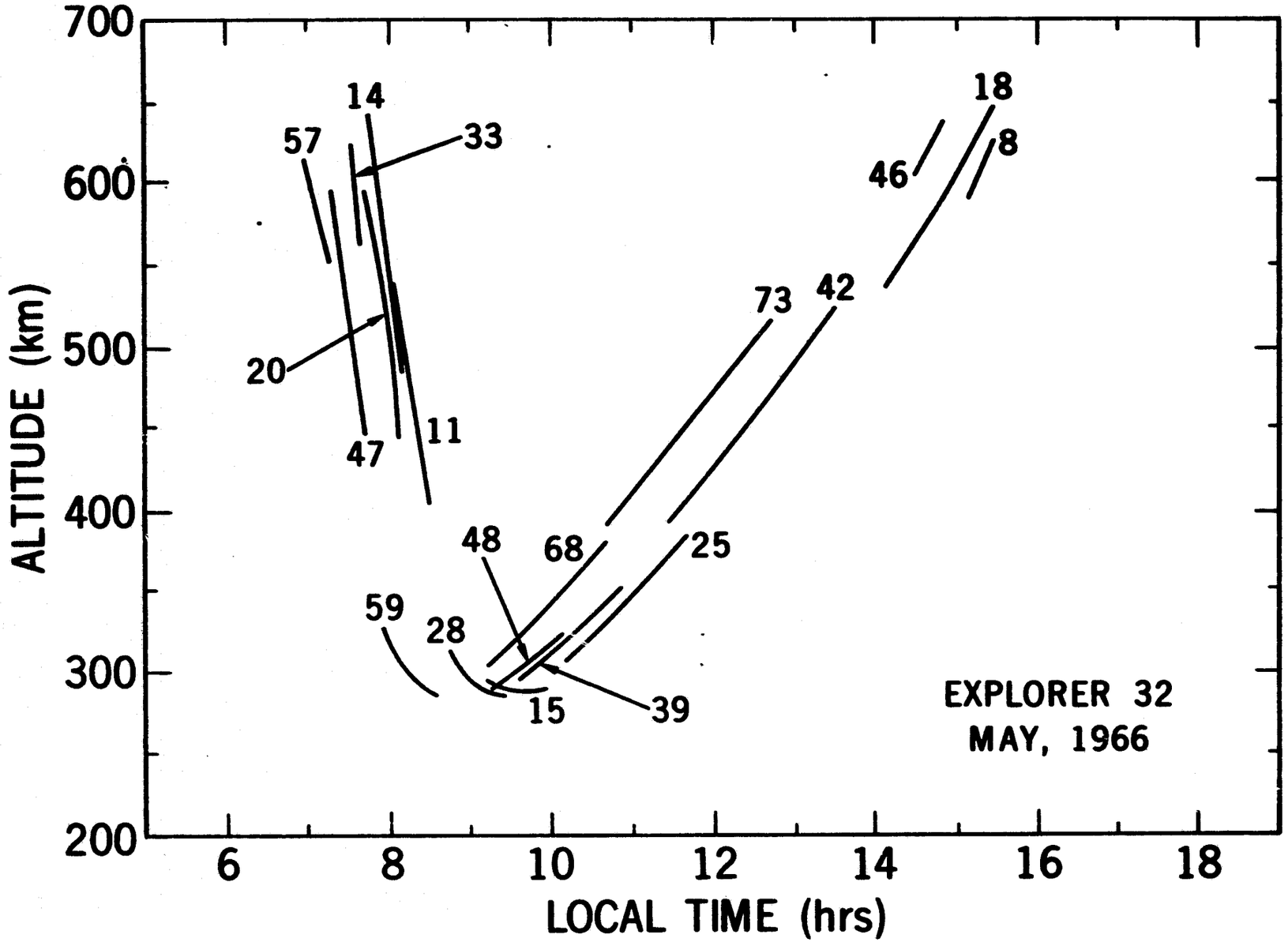

Figure 9. Altitude vs. satellite local time.

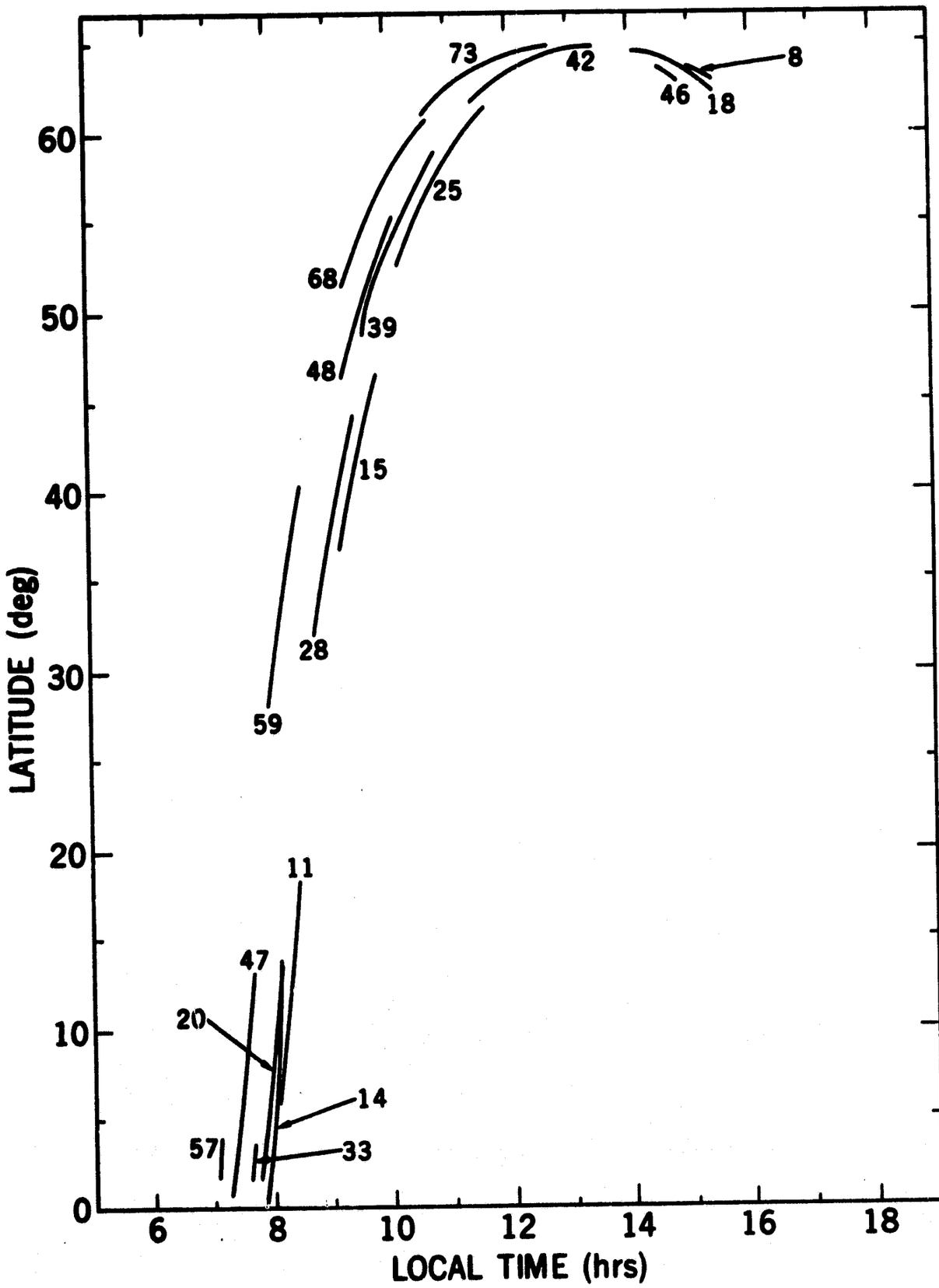

Figure 10. Latitude vs. satellite local time.

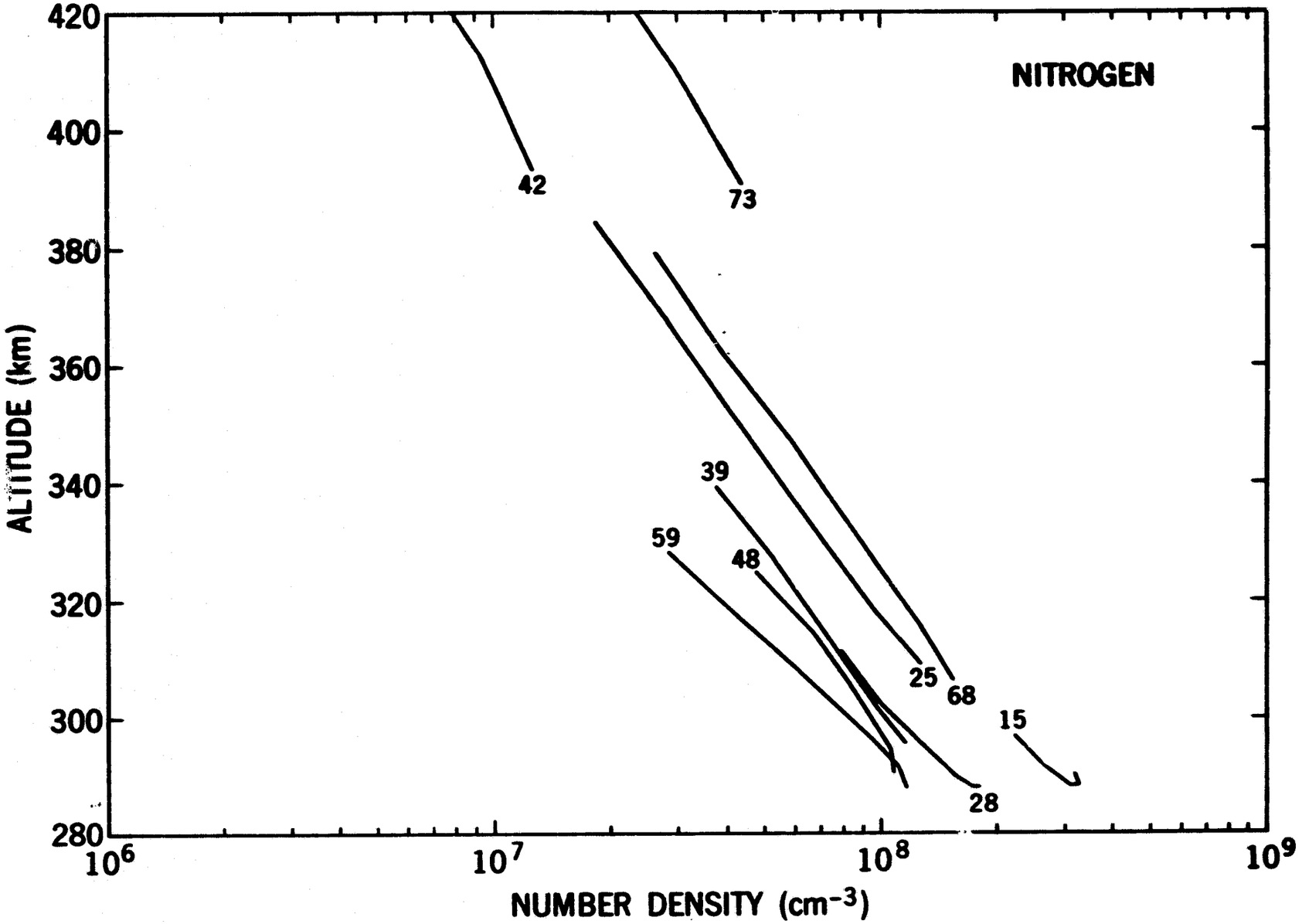

Figure 11a. Average molecular nitrogen number densities from the equatorial and polar mass spectrometers.

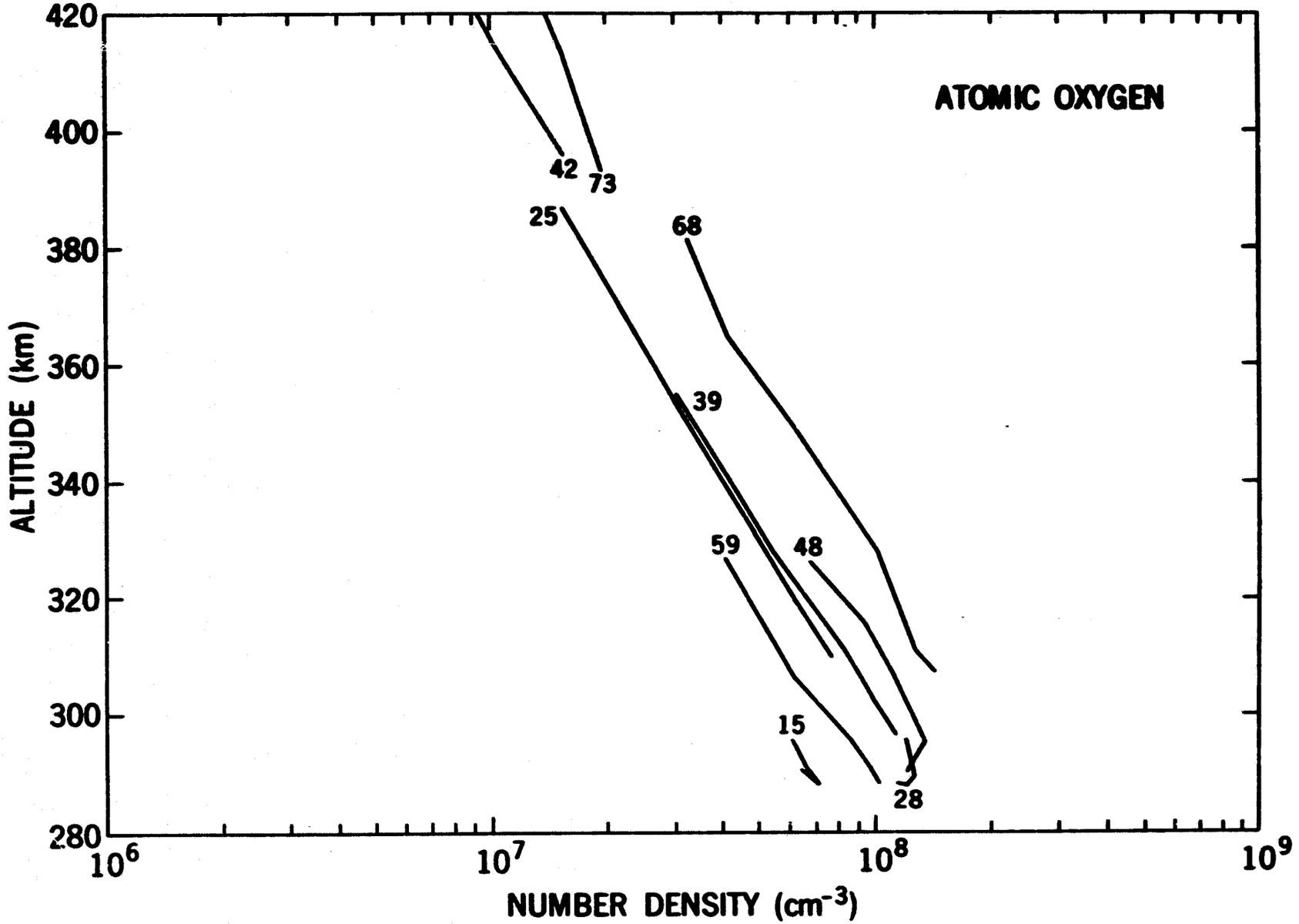

Figure 11b. Average atomic oxygen number densities from the equatorial and polar mass spectrometers.

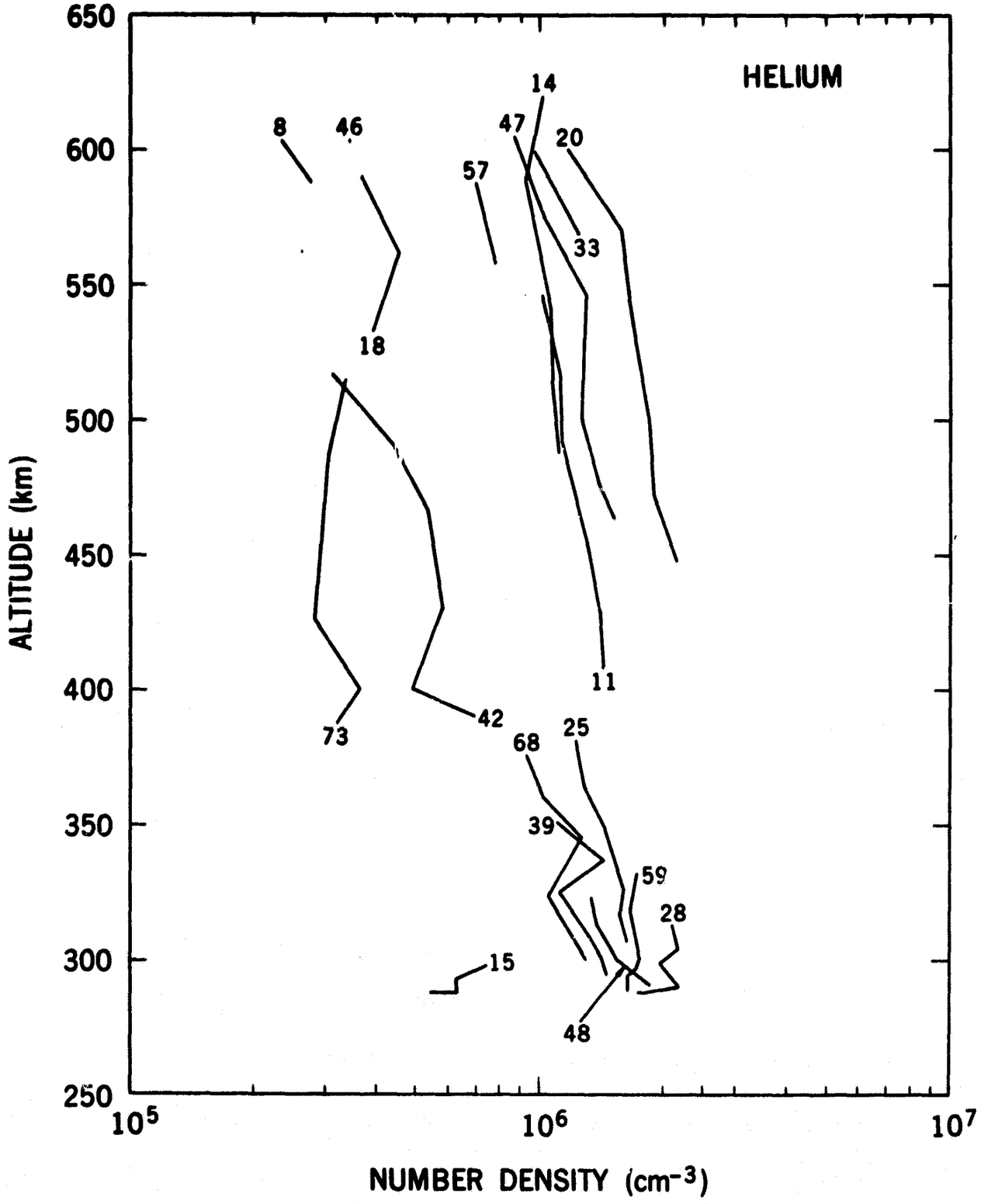

Figure 11c. Average helium number densities from the equatorial and polar mass spectrometers.

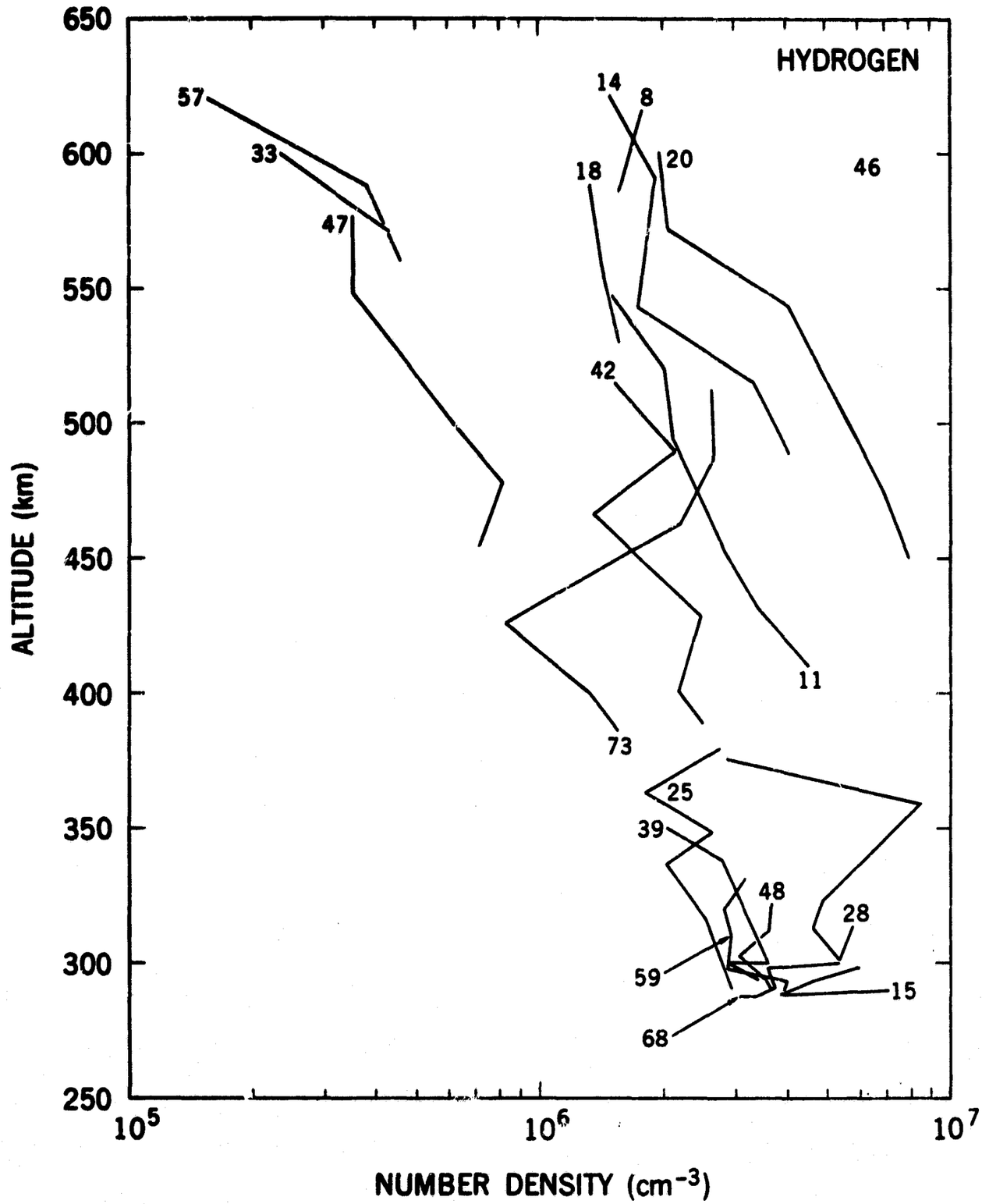

Figure 11d. Average atomic hydrogen number densities from the equatorial and polar mass spectrometers.

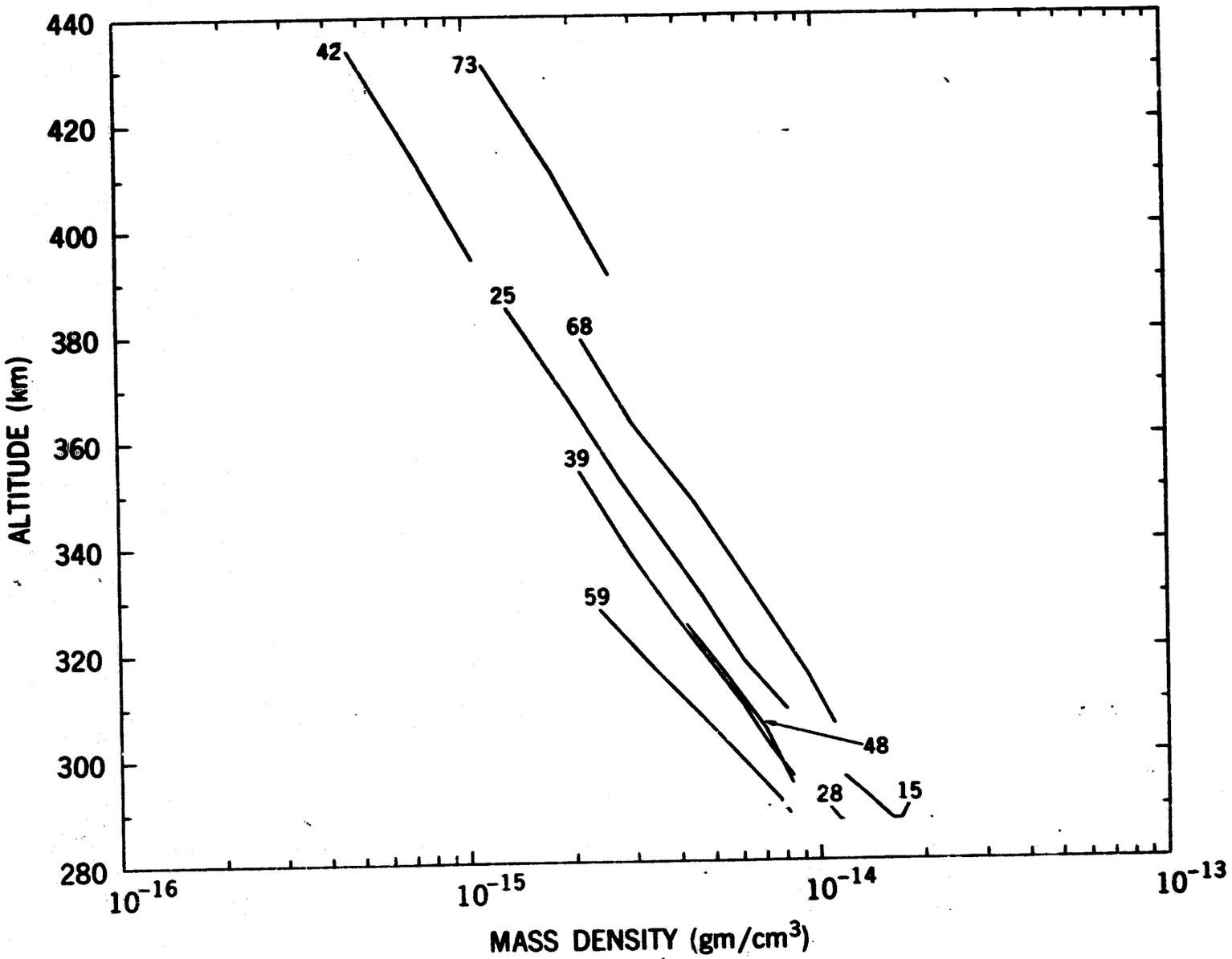

Figure 12. Total mass density obtained from the average number densities of both mass spectrometers.

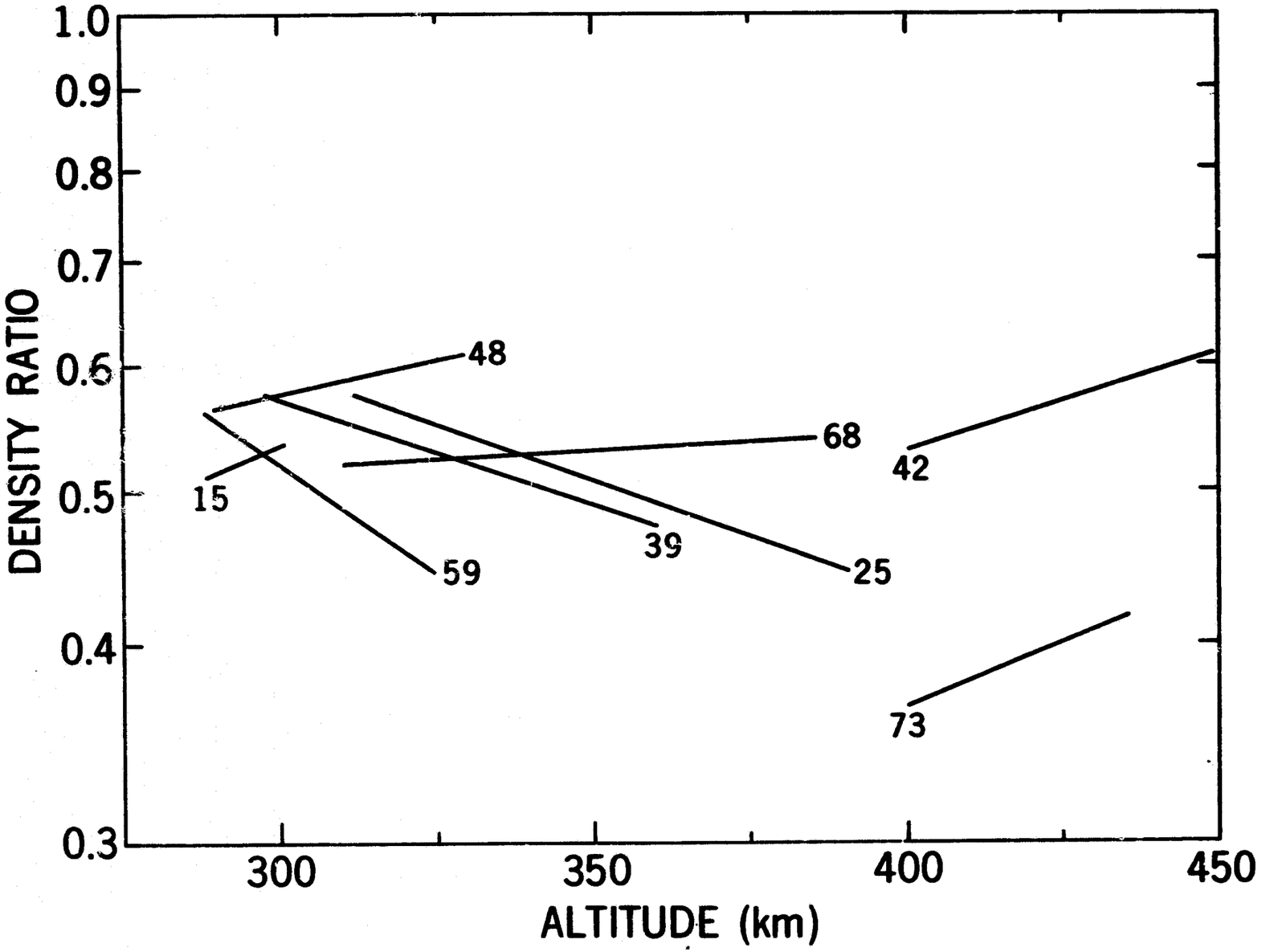

Figure 13. Ratio of total mass density from mass spectrometer to total mass density from pressure gauges on Explorer 32.

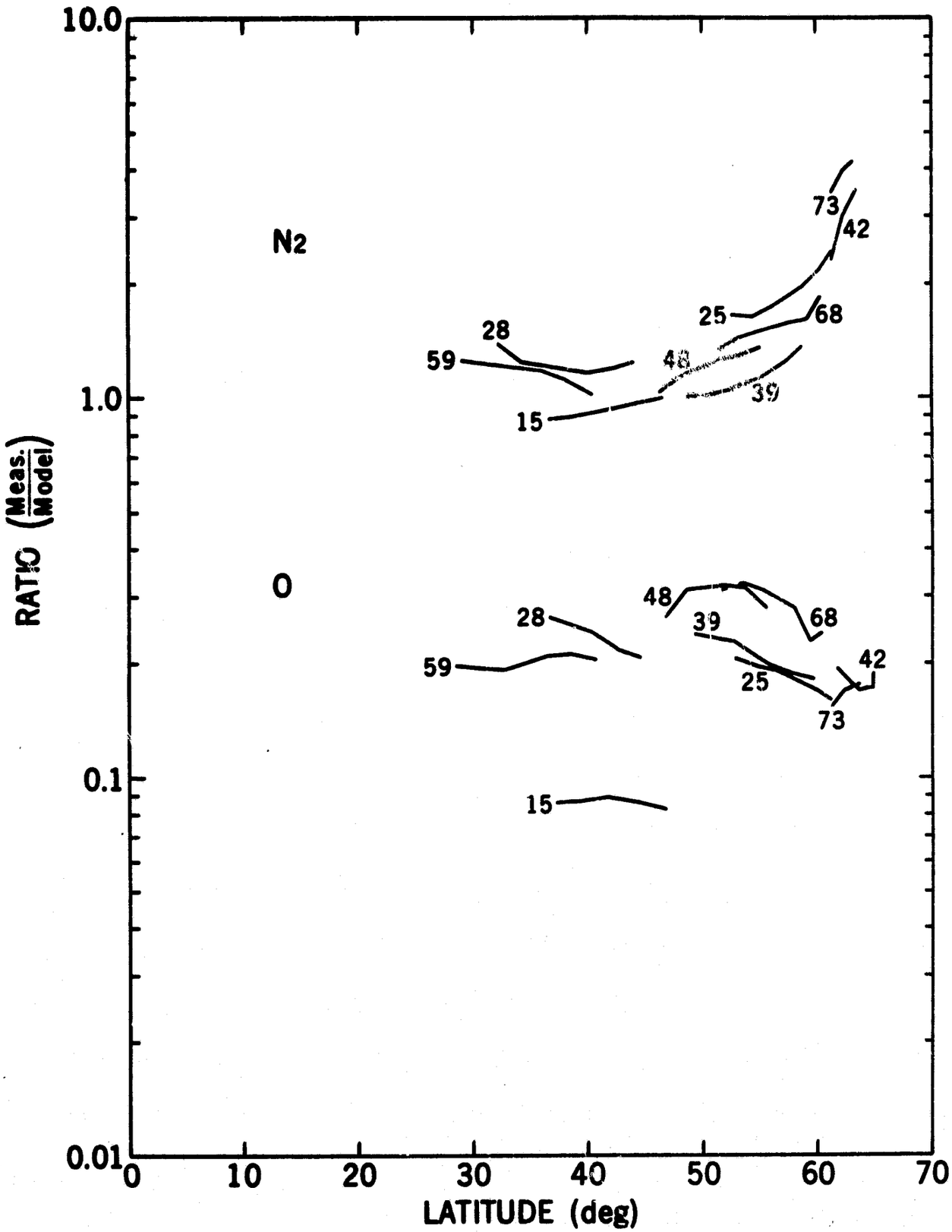

Figure 14a. Ratio of measured number densities to Jacchia 1965 model for molecular nitrogen and atomic oxygen as a function of latitude.

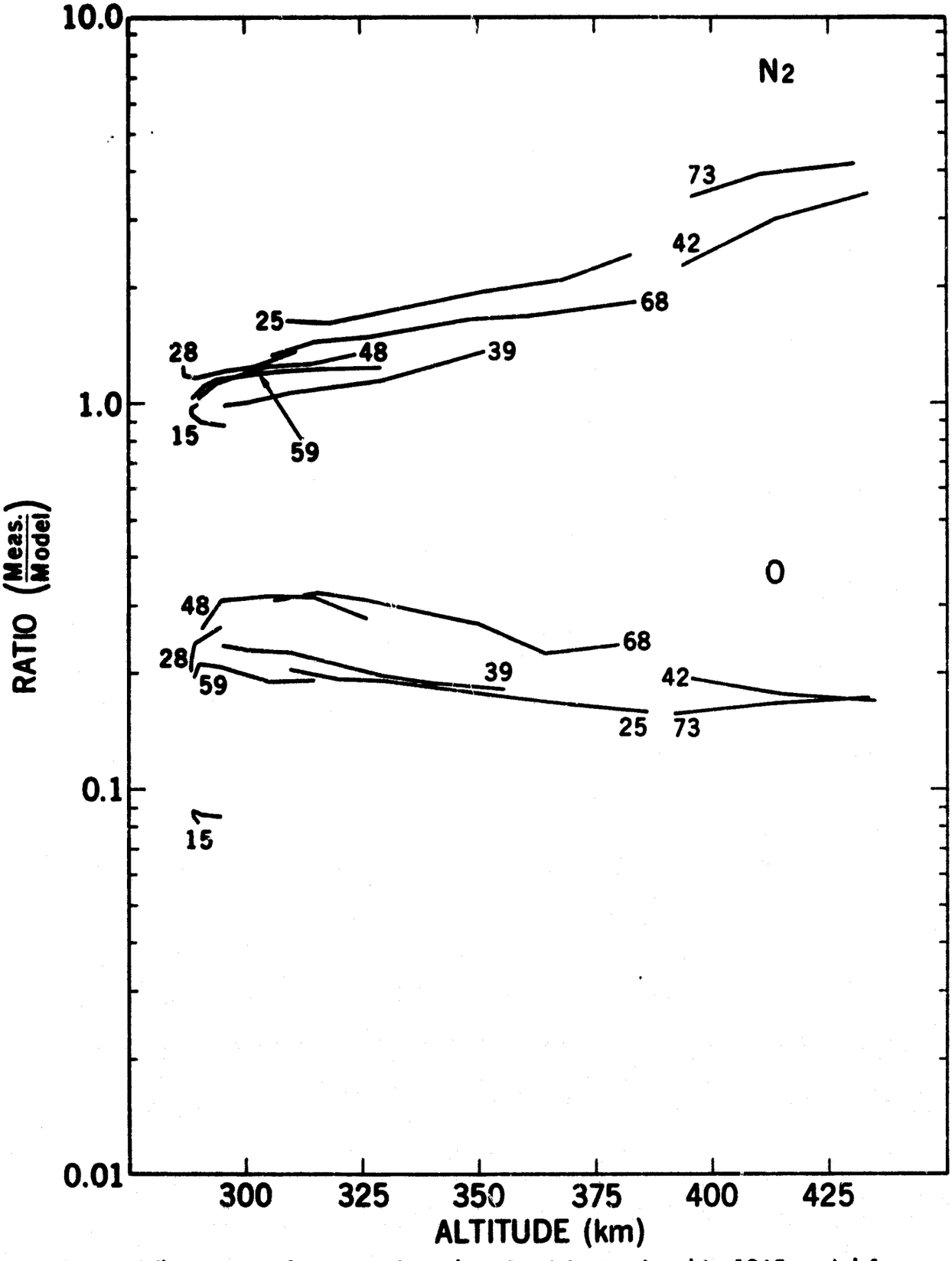

Figure 14b. Ratio of measured number densities to Jacchia 1965 model for molecular nitrogen and atomic oxygen as a function of altitude.

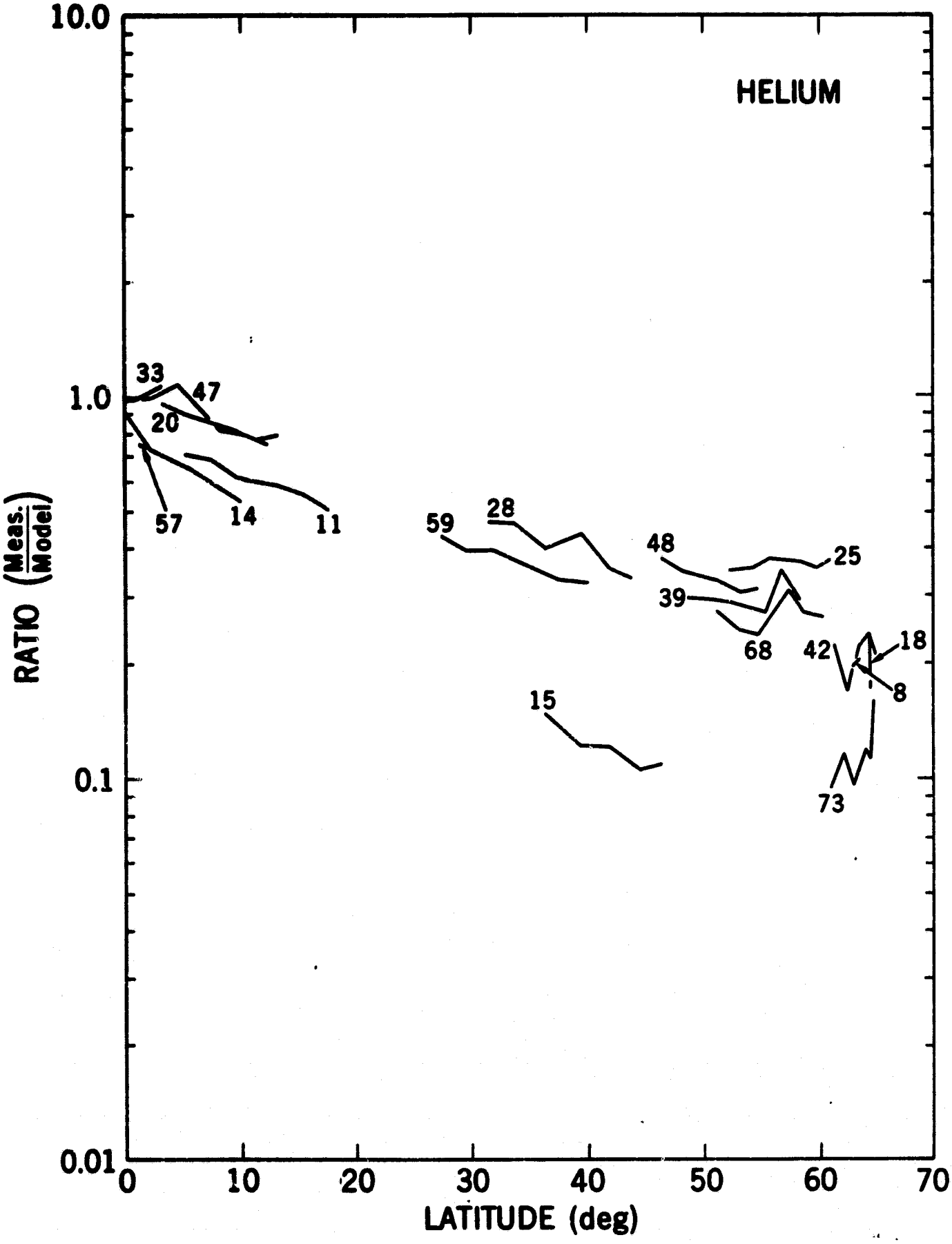

Figure 15. Ratio of measured number densities to Jacchia 1965 model for helium as a function of latitude.

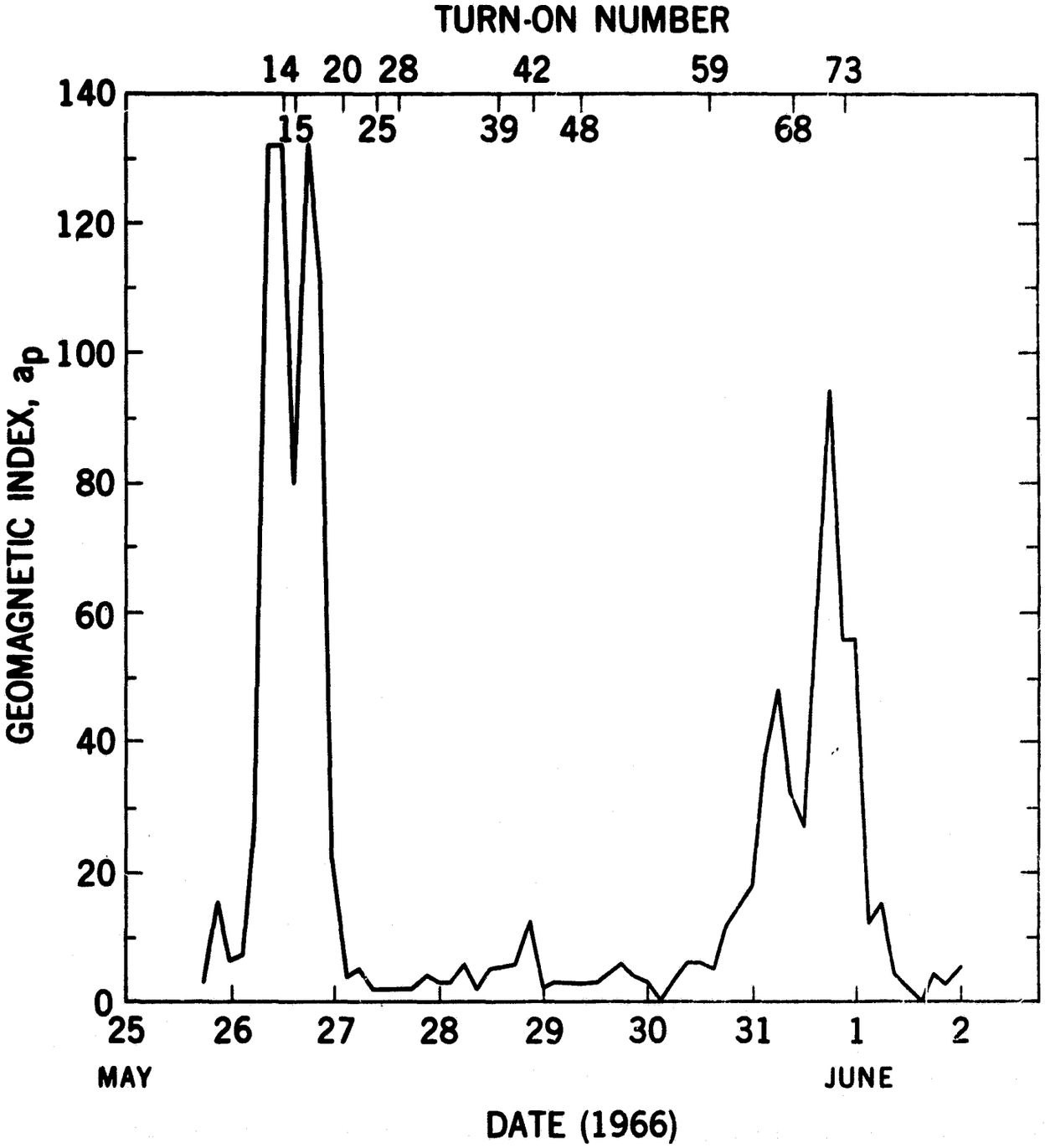

Figure 16. Geomagnetic index, a_p, as a function of day. Also shown are the turn-on numbers.